MedKGent: A Large Language Model Agent Framework for Constructing Temporally Evolving Medical Knowledge Graph

Duzhen Zhang*[1], Zixiao Wang*[1], Zhong-Zhi Li*[2], Yahan Yu[3], Shuncheng Jia[2], Jiahua Dong[1], Haotian Xu[4], Xing Wu[2], Yingying Zhang[5], Tielin Zhang[6], Jie Yang[7], Xiuying Chen†[1], and Le Song †[1,8]

[1]Mohamed bin Zayed University of Artificial Intelligence, Abu Dhabi, UAE
[2]University of Chinese Academy of Sciences, Beijing, China
[3]Kyoto University, Kyoto, Japan
[4]Tsinghua University, Beijing, China
[5]East China Normal University, Shanghai, China
[6]Center for Excellence in Brain Science and Intelligence Technology, Chinese Academy of Sciences, Shanghai, China
[7]Brigham and Women's Hospital, Harvard Medical School, Boston, MA, USA
[8]GenBio AI, San Francisco, USA

Abstract

The rapid expansion of medical literature presents growing challenges for structuring and integrating domain knowledge at scale. Knowledge Graphs (KGs) offer a promising solution by enabling efficient retrieval, automated reasoning, and knowledge discovery. However, current KG construction methods often rely on supervised pipelines with limited generalizability or naively aggregate outputs from Large Language Models (LLMs), treating biomedical corpora as static and ignoring the temporal dynamics and contextual uncertainty of evolving knowledge. To address these limitations, we introduce MedKGent, a LLM agent framework for constructing temporally evolving medical KGs. Leveraging over 10 million PubMed abstracts published between 1975 and 2023, we simulate the emergence of biomedical knowledge via a fine-grained daily time series. MedKGent incrementally builds the KG in a day-by-day manner using two specialized agents powered by the Qwen2.5-32B-Instruct model. The Extractor Agent identifies knowledge triples and assigns confidence scores via sampling-based estimation, which are used to filter low-confidence extractions and inform downstream processing. The Constructor Agent incrementally integrates the retained triples into a temporally evolving graph, guided by confidence scores and timestamps to reinforce recurring knowledge and resolve conflicts. The resulting KG contains 156,275 entities and 2,971,384 relational triples—representing, to our knowledge, the largest LLM-derived medical KG constructed to date. Quality assessments by two state-of-the-art LLMs (GPT-4.1 and DeepSeek-v3) and three domain experts demonstrate an accuracy approaching 90%, with strong inter-rater agreement. To evaluate downstream utility, we conduct retrieval-augmented generation across seven medical question answering benchmarks using five leading LLMs (GPT-4-turbo, GPT-3.5-turbo, DeepSeek-v3, Qwen-Max, and Qwen-Plus), consistently observing significant improvements over non-augmented baselines. Case studies further demonstrate the KG's value in literature-based drug repurposing via confidence-aware causal inference. Collectively, these results establish MedKGent as a scalable, time-sensitive, and trustworthy foundation for medical knowledge representation, with broad applications in clinical decision support, research synthesis, and AI-driven discovery.

*Duzhen Zhang (bladedancer957@gmail.com, duzhen.zhang@mbzuai.ac.ae), Zixiao Wang, and Zhong-Zhi Li contribute equally.
†Corresponding author. Email: le.song@mbzuai.ac.ae and xiuying.chen@mbzuai.ac.ae.

1 Introduction

The rapid expansion of medical literature presents growing challenges for organizing, synthesizing, and accessing clinically relevant knowledge [1]. With millions of publications spanning decades and disciplines, clinicians and researchers increasingly struggle to keep pace with new findings, reconcile conflicting evidence, and extract actionable insights [2]. These challenges highlight the need for scalable methods to transform unstructured text into structured knowledge to support data-driven discovery [3,4]. Knowledge Graphs (KGs) offer a promising solution by converting free text into structured representations that enable machine reasoning and large-scale knowledge integration [5,6]. Represented as relational triples linking biomedical entities and their relationships, KGs capture both semantic content and contextual connections in a graph-based format [7, 8]. They have been applied across diverse biomedical tasks, including drug repurposing, disease–gene association, clinical decision support, and literature-based discovery [9, 10]. By organizing domain knowledge into interpretable and interconnected structures, KGs support automated reasoning, uncover latent associations, and enable downstream applications such as Question Answering (QA) and hypothesis generation [11]. With the growing adoption of Large Language Models (LLMs) in biomedical informatics, KGs are increasingly integrated into LLM workflows to provide structured external knowledge—for example, within Retrieval-Augmented Generation (RAG) frameworks—enhancing factual accuracy, interpretability, and reasoning in knowledge-intensive tasks [12]. Together, these capabilities establish KGs as foundational infrastructure for structuring and leveraging biomedical knowledge at scale [13, 14].

Despite their promise, the automatic construction of KGs from unstructured medical literature remains a formidable challenge, primarily due to the scale, heterogeneity, and linguistic complexity of biomedical texts. Traditional approaches typically rely on multi-stage information extraction pipelines, most commonly involving named entity recognition and relation extraction, to convert free text into structured triples that represent entities and their relations [15, 16]. These pipelines are implemented using either rule-based or learning-based strategies. Rule-based systems depend on expert-defined patterns and domain-specific heuristics [17–23], while learning-based methods, particularly those leveraging machine learning [24–31] and deep learning techniques [32–41], have markedly improved extraction performance by capturing semantic and syntactic structures. Nevertheless, despite these advances, learning-based models exhibit limited generalizability. They typically require large volumes of annotated data for supervised training or fine-tuning [40,41], and their reliance on fixed schema structures impedes the incorporation of novel relation types—often necessitating extensive re-annotation and retraining. As a result, building customized and extensible KGs with minimal human input remains resource-intensive and difficult to scale, posing substantial barriers to scalability and adaptability in dynamic, real-world clinical settings.

In light of these limitations, LLMs, exemplified by GPT-4 [42, 43], have emerged as a promising alternative for KG construction [44–62]. Pretrained on large-scale and diverse textual corpora, LLMs encode broad world knowledge, enabling zero-shot information extraction across domains, including biomedicine, through flexible interfaces with minimal supervision or finetuning [63–66]. Notably, LLMs can accommodate emerging relation types via prompt engineering [67,68], thereby obviating the need for fixed schemas or retraining when confronted with novel medical concepts. These capabilities position LLMs as a scalable, flexible, and data-efficient solution for medical knowledge extraction in complex, information-rich environments.

Despite their advantages, current LLM-based approaches to KG construction frequently treat medical literature as a static corpus—extracting relational triples from all documents simultaneously and aggregating them without regard for temporal context. This often involves taking the union of extracted entities and relations, without considering the specific timeframes in which the knowledge first appeared. As a result, these methods fail to capture the evolving nature of medical knowledge, wherein new evidence may refine, contradict, or reinforce previous findings. In the absence of temporal modeling, such dynamics are effectively lost. Furthermore, most existing approaches lack mechanisms for assigning confidence scores to extracted knowledge [69], thereby limiting their ability to resolve contradictions or reinforce reliably recurrent information. Without modeling temporal progression or epistemic uncertainty, current methods fall short of generating coherent, trustworthy, and dynamically evolving representations of biomedical knowledge.

To address these limitations, we introduce MedKGent, a LLM agent framework for constructing a temporally evolving medical KG. We curated 10,014,314 PubMed abstracts published between January 1, 1975, and December 31, 2023, and organized them into a fine-grained daily time series to preserve the chronological trajectory of biomedical knowledge emergence. In contrast to static approaches, MedKGent processes abstracts incrementally on a day-by-day basis, enabling the KG to evolve dynamically while remaining extensible to future updates. The framework consists of two coordinated agents, both built on the open-source Qwen2.5-32B-Instruct model [70]. The Extractor Agent identifies relational triples from each abstract and assigns initial confidence scores via sampling-based confidence estimation [71–73], which are used to filter low-confidence extractions and guide downstream processing. It also enriches extracted entities and relations with detailed attribute information to support downstream applications such as entity disambiguation and clinical information retrieval. The Constructor Agent integrates the curated triples into a temporal graph through continual interaction with a graph database. Guided by confidence scores and timestamps, it incrementally refines the KG by reinforcing frequently observed knowledge and resolving conflicting relations, thereby maintaining coherence as the literature evolves. The resulting KG contains 156,275 entities and 2,971,384 relational triples—representing, to our knowledge, the largest LLM-derived medical KG constructed to date.

To evaluate the quality of the resulting KG, we conducted both automated and expert assessments. Two state-of-the-art LLMs—GPT-4.1 [74] and DeepSeek-v3 [75], alongside three PhD-level domain experts independently evaluated the extracted triples. All assessments reported high accuracy, approaching 90%, with strong agreement across evaluators, supporting the overall reliability of the KG. To assess downstream utility, we evaluated the KG on seven medical QA datasets, including four widely used benchmarks—MMLU-Med, MedQA-US, PubMedQA*, and BioASQ-Y/N [76]—and three recently released differential diagnosis datasets: MedDDx-Basic, MedDDx-Intermediate, and MedDDx-Expert [77]. Across all tasks, RAG using our KG consistently improved performance for five leading LLMs (GPT-4-turbo [78], GPT-3.5-turbo [78], DeepSeek-v3 [75], Qwen-Max [79], and Qwen-Plus [79]), underscoring its utility as a reliable and clinically relevant knowledge source. Beyond quantitative evaluation, case studies further demonstrated the KG's potential for literature-based drug repurposing. Leveraging temporal and semantic information, we performed confidence-aware causal inference to identify previously unreported *Chemical–Disease* treatment associations. Several predictions—generated without access to future data—were later corroborated by independent publications, highlighting the KG's ability to anticipate emerging therapeutic links and support hypothesis-driven drug repositioning. Collectively, these findings establish MedKGent as a temporally informed, scalable, and trustworthy framework for biomedical knowledge representation, with broad potential to advance clinical decision-making, medical research, and AI-enabled discovery.

2 Results

2.1 Method overview

As illustrated in Figure 1 **a**, we collected over 20 million abstracts from PubMed[1] as the data source for constructing the medical KG, given their concise and information-dense summaries of research findings. These abstracts underwent a series of quality control procedures, including filtering by abstract length (Extended Data Figure 1 **a**) and publication year (Extended Data Figure 1 **b**). The final dataset, comprising 10,014,314 abstracts, was organized into a daily time series from January 1, 1975, to December 31, 2023 (Extended Data Figure 1 **c**), enabling high-resolution temporal analysis.

We introduce MedKGent, a LLM-based agent framework designed to construct a temporally evolving medical KG. The framework processes biomedical abstracts sequentially from January 1, 1975, to December 31, 2023, enabling incremental KG growth while ensuring adaptability for future updates. MedKGent comprises two coordinated agents—the Extractor Agent and the Constructor Agent—deployed via a self-hosted API using the open-source Qwen2.5-32B-Instruct model [70]. As shown in Figure 1 **b**, for a given biomedical abstract (*e.g.*, PubMed ID 10494624), the Extractor Agent first utilizes the PubTator3 tool [80] to identify entities across six categories: Gene, Disease, Chemical, Variant, Species, and CellLine. This tool extracts entities, assigns types, and normalizes synonymous mentions with unique identifiers, facilitating entity disambiguation and retrieval—key steps for accurate KG construction. For example, "NPPA" is classified as a Gene with identifier "4878" and terminology "NCBI Gene". Moreover, the Extractor Agent enriches each entity with Exact Keywords (standardized to lowercase and mapped to a single identifier, *e.g.*, aliases: "anp", "atrial np", and "nppa" for "NPPA") and Semantic Embedding attributes—a vector generated by BiomedBERT [81] to capture semantic context. These enriched representations enhance retrieval precision and efficiency, particularly when explicit identifiers are unavailable.

Next, the Extractor Agent uses the abstract and extracted entities to prompt the LLM, inferring semantic relationships between entity pairs (prompt shown in Extended Data Figure 2 **a**). We define 12 core biomedical relation types: seven bidirectional (Associate, Negative Correlate, Positive Correlate, Compare, Cotreat, Interact, Drug Interact) and five unidirectional (Cause, Inhibit, Treat, Stimulate, Prevent), as detailed in Extended Data Figure 2 **d**. These relations can be flexibly extended by prompt design, enabling MedKGent to incorporate emerging medical relations with minimal manual intervention, eliminating the need for rigid schemas or retraining typically required in supervised pipelines. Inspired by the self-consistency principle [71–73], the Extractor Agent uses sampling-based confidence estimation to assign an initial confidence score to each triple. For a given extraction prompt, the Extractor Agent performs multiple parallel LLM inferences, calculating the frequency of each triple across outputs

[1] https://pubmed.ncbi.nlm.nih.gov/

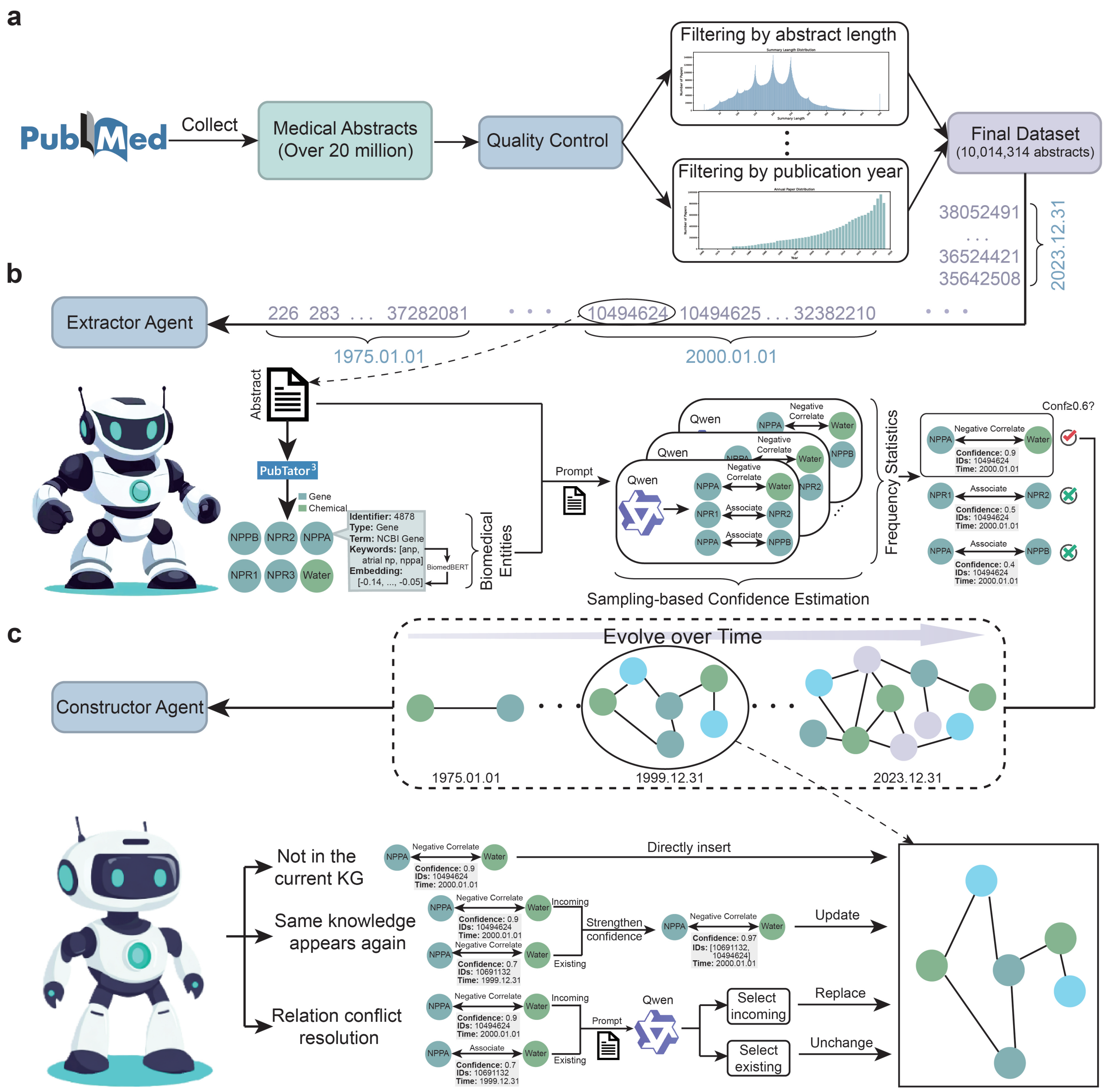

Figure 1: Overview of the MedKGent framework for constructing a temporally evolving medical KG. **a**. Data collection and preprocessing pipeline. Over 20 million PubMed abstracts were retrieved and subjected to quality control, including filtering by abstract length and publication year, yielding 10,014,314 abstracts organized as a daily time series from 1975–2023 to enable fine-grained temporal analysis. **b**. Entity and relation extraction by the Extractor Agent. Each biomedical abstract is processed using PubTator3 to detect and normalize entities across six biomedical categories. Entities are enriched with exact keywords and semantic embeddings, followed by LLM-based inference of biomedical relations with sampling-based confidence estimation; low-confidence triples are discarded. **c**. Incremental graph construction by the Constructor Agent. High-confidence triples are integrated into the evolving KG, with confidence scores strengthened when re-encountered, PubMed IDs appended for provenance, and timestamps refreshed. Conflicting relations are resolved through LLM-based reasoning, ensuring consistent and temporally aware knowledge integration.

as its confidence score. For instance, if the triple (NPPA, Negative Correlate, Water) appears in 90% of the outputs, its confidence score is 0.9. Low-confidence triples (score$<$0.6) are filtered out, and only high-confidence triples are retained for downstream graph construction. Each triple is also annotated with the PubMed ID of the source abstract and a timestamp, ensuring traceability and source attribution. For example, (NPPA, Negative Correlate, Water) would have a PubMed ID of 10494624 and a timestamp of 2000-01-01.

As shown in Figure 1 **c**, for each retained triple, such as (NPPA, Negative Correlate, Water), the Constructor Agent checks its presence in the current KG. If absent (*i.e.*, either the head or tail entities are missing), it is inserted; if present, its confidence score is updated according to Equation (1). The associated PubMed ID is appended, and the timestamp is updated to reflect the latest publication. For example, if an existing triple (NPPA, Negative Correlate, Water) has a confidence score of 0.7, PubMed ID 10691132, and timestamp 1999-12-31, and a new occurrence with a confidence score of 0.9, PubMed ID 10494624, and timestamp 2000-01-01 is encountered, the updated triple will have a confidence score of 0.97, PubMed IDs [10691132, 10494624], and a timestamp of 2000-01-01. If the head and tail entities are present but the relation differs, such as existing (NPPA, Associate, Water) vs. incoming (NPPA, Negative Correlate, Water), only the most appropriate relation is maintained. The Constructor Agent invokes the LLM to resolve the conflict by selecting the more suitable relation, considering both the existing and incoming triple's confidence scores and timestamps. If the LLM selects the new triple, the existing one is replaced; otherwise, no changes are made. The prompt design for relation conflict resolution is shown in Extended Data Figure 2 **c**. Together, the two agents extract structured medical facts and integrate them into a dynamic, time-aware KG. See more details in the Section 4.

2.2 Structural Characterization of the Knowledge Graph

In this section, we detail the structural characteristics of the medical KG we constructed, with an emphasis on the distribution of node types, relationship types, and the confidence scores of relationship triples. We also present a visualization of a subgraph centered on COVID-19 to illustrate the graph's structure.

Using the MedKGent framework, we extracted knowledge triples from the abstracts of 10,014,314 medical papers, with 3,472,524 abstracts (34.68%) yielding extractable triples. The relatively low extraction rate can be attributed to several factors: first, some abstracts lacked sufficient structured information for triple extraction; second, only triples with a confidence score exceeding 0.6 were retained, excluding those with lower confidence; and third, some triples extracted by LLMs contained formatting issues, such as extraneous or irrelevant characters, which were discarded. In total, our Extractor Agent identified 8,922,152 valid triples from the abstracts. However, the extracted triples contained a significant number of duplicates and conflicts. To resolve this, our Constructor Agent integrates the triples in chronological order. During this process, duplicates are merged, with the confidence score for each triple increasing in proportion to its frequency, reflecting greater certainty. For conflicting triples, where the same entity pair is associated with multiple relations, the Constructor Agent retains the most appropriate relationship. Following this consolidation, the final KG comprises 2,971,384 distinct triples.

We conducted a comprehensive statistical analysis of the final constructed KG, which comprises 156,275 nodes. As shown in Figure 2 **a**, the node distribution is predominantly dominated by Gene and Chemical nodes, with smaller proportions of other entities such as Disease, Variant, Species, and CellLine. The KG includes 2,971,384 relationship triples (edges), representing a range of interactions between entities, as illustrated in Figure 2 **b**. The most common relationship type is "Associate", followed by "Negative Correlate" and "Positive Correlate", indicating strong associations between medical entities. Less frequent relationships, such as "Interact", "Prevent", and "Drug_Interact", provide additional insights into the complexities of medical interactions. The distribution of confidence scores for these relationship triples, shown in Figure 2 **c**, with confidence values discretized to the nearest smaller 0.05 increment (rounding down to the closest multiple of 0.05), reveals a clear dominance of high-confidence triples. A significant proportion of triples exhibit confidence scores of 0.95, reflecting the cumulative increase in confidence resulting from the repetition of triples during the graph construction process. This high-confidence distribution reinforces the reliability and robustness of the KG.

We visualized a local subgraph of the constructed KG with COVID-19 as the central node, highlighting five surrounding relationship triples, as shown in Figure 2 **d**. Each node is characterized by six key attributes: the Identifier, which uniquely references the node and normalizes multiple synonymous mentions to a standardized terminology entry; the Entity Type, which classifies the entity; the Terminology, which maps the entity type to its corresponding standard terminology; the Page Link, providing a reference to the entity in the Terminology; the Exact Keywords, which lists common names and aliases of the entity in lowercase; and the Semantic Embedding, a vector representation of the entity. In practice, these attributes facilitate entity linking within a query by matching entities to their corresponding nodes in the KG. When the Identifier of an entity in the query is available, entity linking can be efficiently performed using this unique reference. In the absence of an Identifier, precise matching

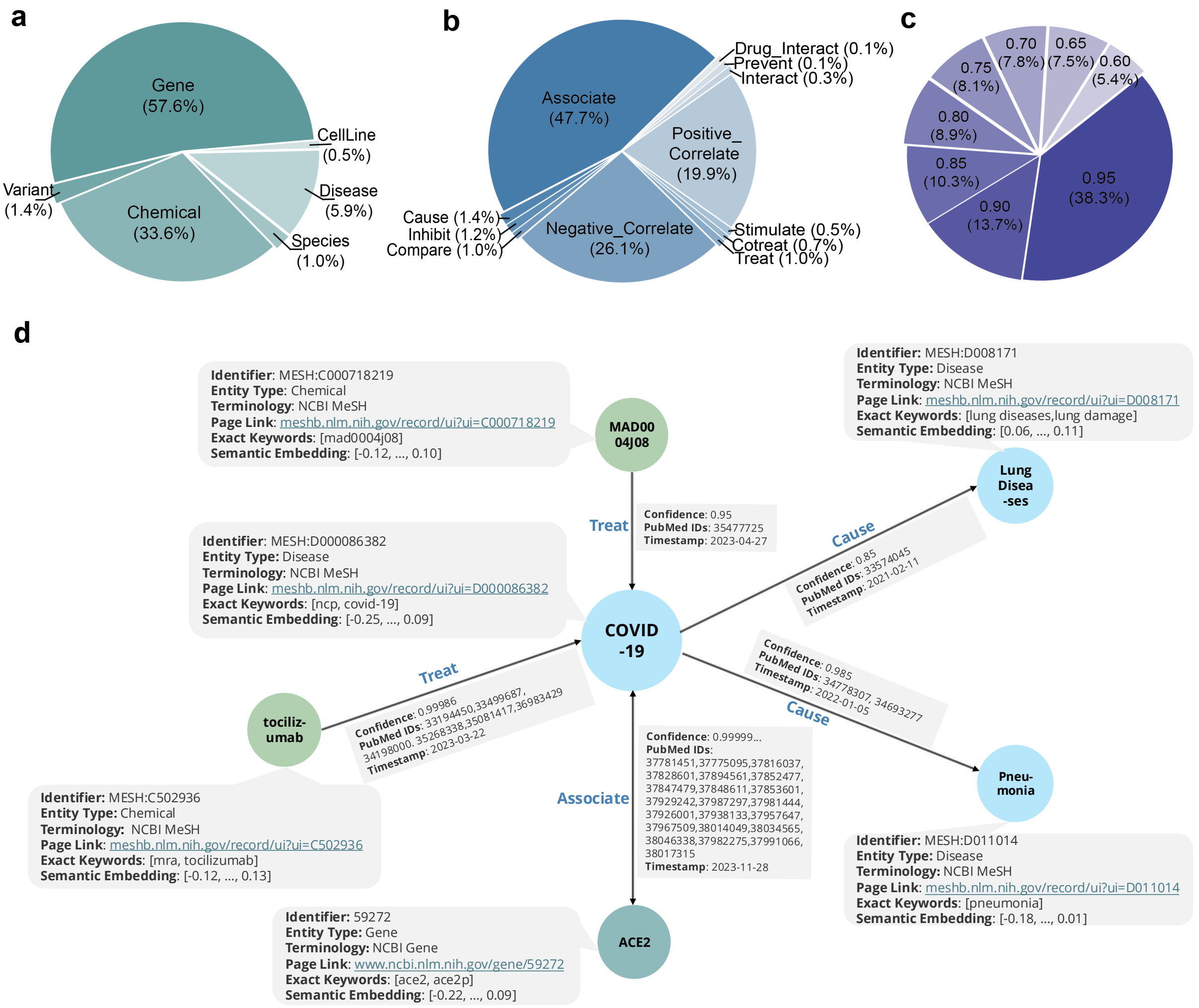

Figure 2: A comprehensive statistical analysis and visualization of the constructed KG, consisting of 156,275 nodes and 2,971,384 relationship edges. **a**. Node distribution within the KG, with Gene and Chemical nodes predominating, and smaller proportions of Disease, Variant, Species, and CellLine. **b**. Relationship type distribution within the KG, highlighting the prevalence of "Associate" relationships, followed by "Negative Correlate" and "Positive Correlate", with less common interactions such as "Interact", "Prevent", and "Drug_Interact". **c**. The distribution of confidence scores for relationship triples, discretized to the nearest smaller 0.05 increment, ensures values are rounded down to the closest multiple of 0.05. This distribution reveals a clear dominance of high-confidence triples, particularly those with scores of 0.95, underscoring the robustness of the KG. **d**. Local subgraph visualization centered on COVID-19, displaying five surrounding relationship triples. Each node is characterized by key attributes, including Identifier, Entity Type, Terminology, Page Link, Exact Keywords, and Semantic Embedding, facilitating efficient entity linking through exact or similarity matching. The relationships in the KG are further enriched by attributes such as Confidence, PubMed IDs, and Timestamp, enhancing traceability, accuracy, and temporal relevance.

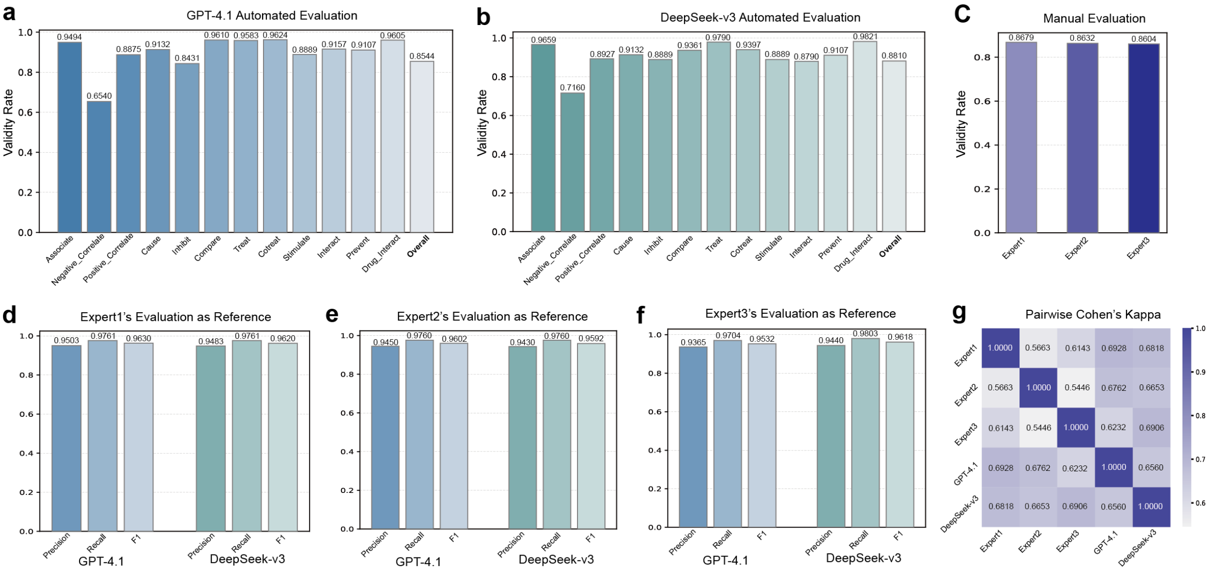

Figure 3: Comprehensive evaluation of extraction quality for relationship triples generated by the Extractor Agent. Systematic assessment of extraction accuracy using both automated evaluations by LLMs and independent manual expert review. **a**. Proportion of valid relationship triples (score ≥2.0) across relation types, as assessed by GPT-4.1 on a randomly selected subset of 34,725 abstracts (83,438 triples). **b**. Proportion of valid relationship triples across relation types, as assessed by DeepSeek-v3 on the same subset. **c**. Validity rates from independent manual evaluation by three domain experts on a subset of 400 abstracts (1,060 triples), demonstrating high inter-expert consistency. **d-f**. Performance of GPT-4.1 and DeepSeek-v3 compared to three expert evaluations on the shared evaluation subset, reporting precision, recall, and F1 score. **g**. Pairwise inter-rater agreement between experts and LLMs quantified by Cohen's kappa coefficients, demonstrating substantial consistency across all evaluators.

is achieved by checking whether the entity appears in the Exact Keywords list of a specific node. Alternatively, semantic vectors of the query entities can be compared with those in the KG to identify the most similar entities, enabling semantic similarity matching. This approach is particularly beneficial for entities with multiple names, ensuring accurate linking even when not all aliases are captured in the Exact Keywords list.

The relationships between entities are characterized by three key attributes. Confidence reflects the reliability of the relationship, with higher values indicating greater certainty based on its frequency across multiple sources. The PubMed IDs attribute lists the PubMed identifiers of the papers from which the relationship is derived, enabling easy access to the original publications via the PubMed website[2]. If the relationship appears in multiple papers, all relevant PubMed IDs are included, further increasing the confidence score. Finally, Timestamp denotes the most recent occurrence of the relationship, specifically the publication date of the latest paper. Notably, while Timestamp captures only the latest appearance, the full temporal span of the relationship—including its earliest mention—can be readily retrieved through the associated PubMed IDs via the PubMed website. These attributes collectively enhance the traceability, accuracy, and temporal relevance of the relationships within the KG.

2.3 Quality Assessment of Extracted Relationship Triples

To systematically evaluate the reliability of the Extractor Agent, which generated relationship triples from 3,472,524 abstracts, we conducted both automated and manual assessments to characterize extraction accuracy.

For automated evaluation, two state-of-the-art LLMs, GPT-4.1 [74] and DeepSeek-v3 [75], were employed. A random subset comprising 1% of the abstracts (n = 34,725), resulting in 83,438 extracted triples, was selected for evaluation. Each abstract and its corresponding triples were formatted into structured prompts and independently assessed by both models according to a standardized four-tier rubric: Correct (3.0), Likely Correct (2.0), Likely Incorrect (1.0), and Incorrect (0.0) (the specific evaluation prompt is illustrated in Extended Data Figure 3 **a**). Triples receiving scores of ≥ 2.0 were deemed valid. The evaluation outcomes are presented in Figure 3 **a** and **b**, illustrating the proportion of valid triples across relation types for GPT-4.1 and DeepSeek-v3, respectively. Both models demonstrated high overall accuracy, with 85.44% and 88.10% of triples rated as valid by

[2] https://pubmed.ncbi.nlm.nih.gov/

GPT-4.1 and DeepSeek-v3, respectively. For most relation types, validity was approximately 90%, except for Negative_Correlate, which exhibited slightly lower agreement. These findings underscore the high precision of the Extractor Agent across diverse biomedical relation types and support its utility for downstream analyses.

In parallel, a manual evaluation was conducted to further validate extraction accuracy. Three domain experts with doctoral-level training in artificial intelligence and medicine independently reviewed a randomly selected subset of 400 abstracts, comprising 1,060 extracted triples. Each abstract and its associated triples were evaluated using the same standardized scoring rubric. Triples receiving scores of $\geq$2.0 were considered valid. As shown in Figure 3 **c**, all three reviewers demonstrated high consistency, with overall validity rates exceeding 86% across assessors. The close concordance between manual and automated evaluations further substantiates the robustness of the Extractor Agent in accurately capturing biomedical relationships, providing strong support for the application of the extracted knowledge in large-scale medical analyses.

To further validate the reliability of the LLM-based assessments, we used three expert annotations as reference standards to evaluate GPT-4.1 and DeepSeek-v3 on the same subset of 400 abstracts, respectively. As shown in Figure 3 **d**–**f**, both models exhibited strong concordance with expert evaluations, achieving precision, recall, and F1 scores of approximately 95% across metrics. These results further corroborate the accuracy of the automated scoring framework and its alignment with expert judgment.

Finally, inter-rater agreement was assessed across all evaluators—including three human experts and two LLMs—by computing pairwise Cohen's kappa coefficients on a shared evaluation subset (Figure 3 **g**) [82]. Most pairwise comparisons (80%) yielded kappa values exceeding 0.6, indicating substantial agreement—an accepted threshold for reliable concordance in domains involving subjective judgment, including medicine, psychology, and natural language processing [83]. The coefficients between expert 1 and expert 2 (0.5663), and between expert 2 and expert 3 (0.5446), fell slightly below this threshold but still reflected moderate agreement, closely approaching the substantial range. These findings demonstrate strong inter-rater reliability across both human and automated evaluators, underscoring the robustness and reproducibility of the evaluation framework.

2.4 Evaluating Downstream Utility in Medical Question Answering

We evaluated the downstream utility of our constructed KG as a RAG information source across seven multiple-choice medical QA datasets. These included four widely used benchmarks [76]—MMLU-Med, MedQA-US, PubMedQA*, and BioASQ-Y/N—spanning a broad spectrum of clinical and biomedical reasoning tasks. To further assess diagnostic reasoning under varying complexity, we introduce MedDDx, a newly developed benchmark suite focused on differential diagnosis [77]. Questions are stratified into three levels—MedDDx-Basic, MedDDx-Intermediate, and MedDDx-Expert—based on the variance in semantic similarity among answer choices. All MedDDx subsets were designed to reduce training data leakage and more closely reflect authentic clinical reasoning. Detailed dataset statistics are shown in Figure 4 **a**. We systematically evaluated five state-of-the-art LLMs to measure the impact of KG-based retrieval. Each model was tested in a zero-shot setting under two conditions: (1) direct answering using internal knowledge alone, and (2) RAG, with relevant KG subgraphs prepended as external context. The models—GPT-4-turbo, GPT-3.5-turbo (OpenAI) [78], DeepSeek-v3 (DeepSeek) [75], Qwen-Max, and Qwen-Plus (Qwen) [79]—span diverse architectures and training regimes, representing both proprietary and open-source systems. All models were accessed via publicly available APIs without additional fine-tuning. Version details and access endpoints are summarized in Figure 4 **b**.

Figures 4 **c**-**i** present model performance across the seven medical QA datasets using radar plots, each depicting the five LLMs under both direct answering (w/o RAG) and RAG conditions (w/ RAG). Notably, the background shading in the radar plots is lighter for the MedDDx suite (Figure 4 **g**-**i**) than for the four widely used benchmarks (Figure 4 **c**-**f**), reflecting the overall lower accuracy of all models on these recently introduced and semantically more challenging datasets. This contrast highlights the greater complexity and reduced risk of training data leakage inherent to the MedDDx design. Across all datasets, RAG with our KG consistently outperformed direct answering. The most substantial improvements were observed in tasks requiring deeper clinical reasoning, such as MedQA-US and the MedDDx suite. For example, on MedQA-US, GPT-3.5-turbo improved from 0.5986 to 0.6834 (+8.5 percentage points), and Qwen-Max from 0.7306 to 0.7636. On MedDDx-Expert, RAG yielded absolute gains of up to +8.6 points for GPT-3.5-turbo and +5.7 points for Qwen-Max. Even in knowledge-intensive but semantically simpler tasks such as MMLU-Med and BioASQ-Y/N, RAG offered modest yet consistent benefits. On MMLU-Med, GPT-4-turbo improved from 0.8724 to 0.9054, while DeepSeek-v3 achieved the highest score overall at 0.9183 with KG support. In BioASQ-Y/N, RAG further enhanced already strong performance, with four models exceeding 0.85 accuracy following augmentation. Notably, several models performed better on MedDDx-Expert than on MedDDx-Basic, despite the former being constructed with higher semantic complexity. This counterintuitive trend may be related to differences in distractor framing, where Expert-level distractors—

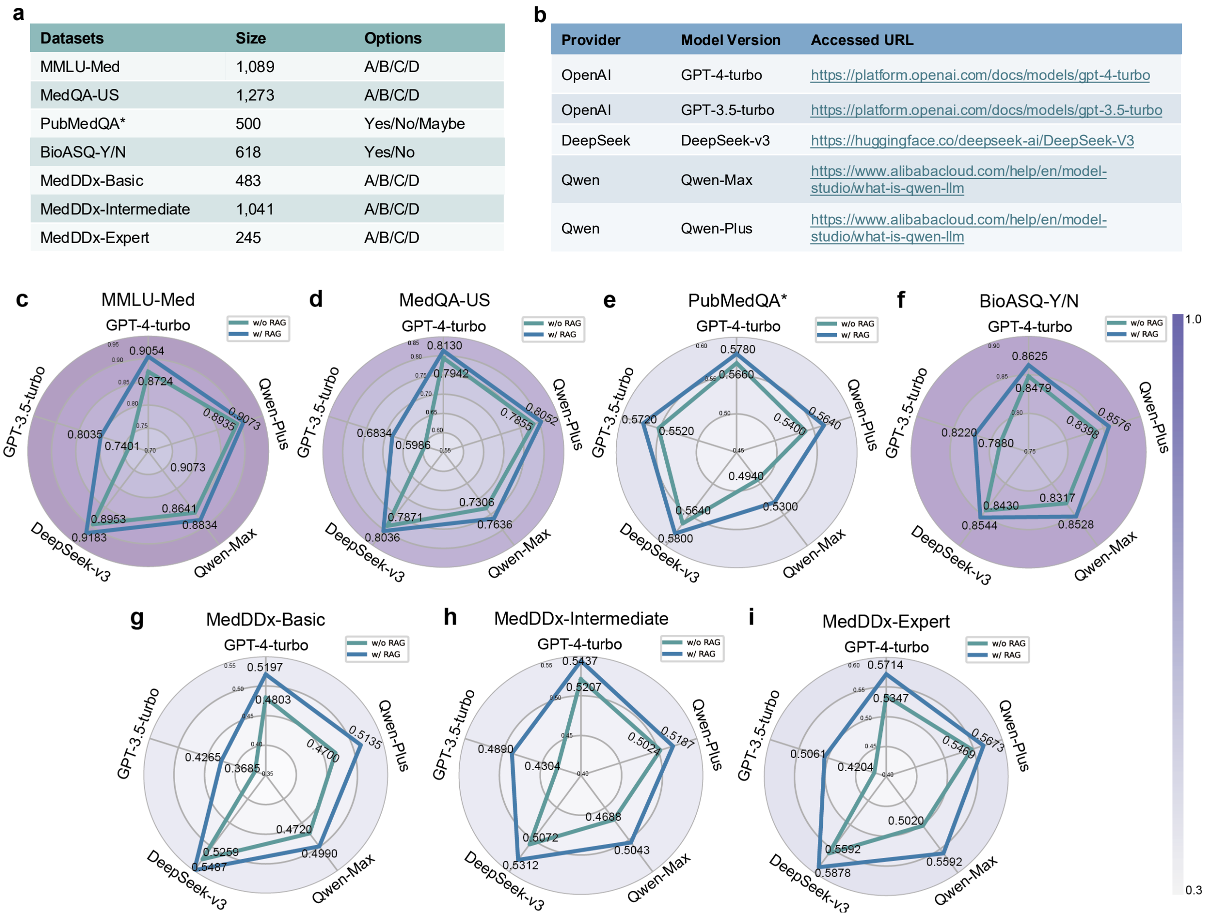

Datasets	Size	Options
MMLU-Med	1,089	A/B/C/D
MedQA-US	1,273	A/B/C/D
PubMedQA*	500	Yes/No/Maybe
BioASQ-Y/N	618	Yes/No
MedDDx-Basic	483	A/B/C/D
MedDDx-Intermediate	1,041	A/B/C/D
MedDDx-Expert	245	A/B/C/D

Provider	Model Version	Accessed URL
OpenAI	GPT-4-turbo	https://platform.openai.com/docs/models/gpt-4-turbo
OpenAI	GPT-3.5-turbo	https://platform.openai.com/docs/models/gpt-3.5-turbo
DeepSeek	DeepSeek-v3	https://huggingface.co/deepseek-ai/DeepSeek-V3
Qwen	Qwen-Max	https://www.alibabacloud.com/help/en/model-studio/what-is-qwen-llm
Qwen	Qwen-Plus	https://www.alibabacloud.com/help/en/model-studio/what-is-qwen-llm

Figure 4: Overview of evaluation datasets, model configurations, and performance across medical QA tasks. **a**. Dataset statistics for the seven medical QA benchmarks used in this study. The benchmark suite includes four widely adopted datasets [76] (MMLU-Med, MedQA-US, PubMedQA*, and BioASQ-Y/N) and three newly developed differential diagnosis datasets [77] (MedDDx-Basic, MedDDx-Intermediate, and MedDDx-Expert). For each dataset, we report the number of multiple-choice questions and the corresponding answer option formats. **b**. Configuration of the five LLMs evaluated: GPT-4-turbo, GPT-3.5-turbo (OpenAI) [78], DeepSeek-v3 (DeepSeek) [75], Qwen-Max, and Qwen-Plus (Qwen) [79]. All models were accessed through public APIs in their zero-shot settings without fine-tuning. The specific version identifiers and access platforms are indicated. **c**-**i**. Model performance across the seven QA datasets, shown as radar plots. Each chart compares zero-shot accuracy for five LLMs under two conditions: direct answering without retrieval (w/o RAG) and RAG with our KG (w/ RAG). Across all datasets, RAG with our KG consistently outperformed direct answering.

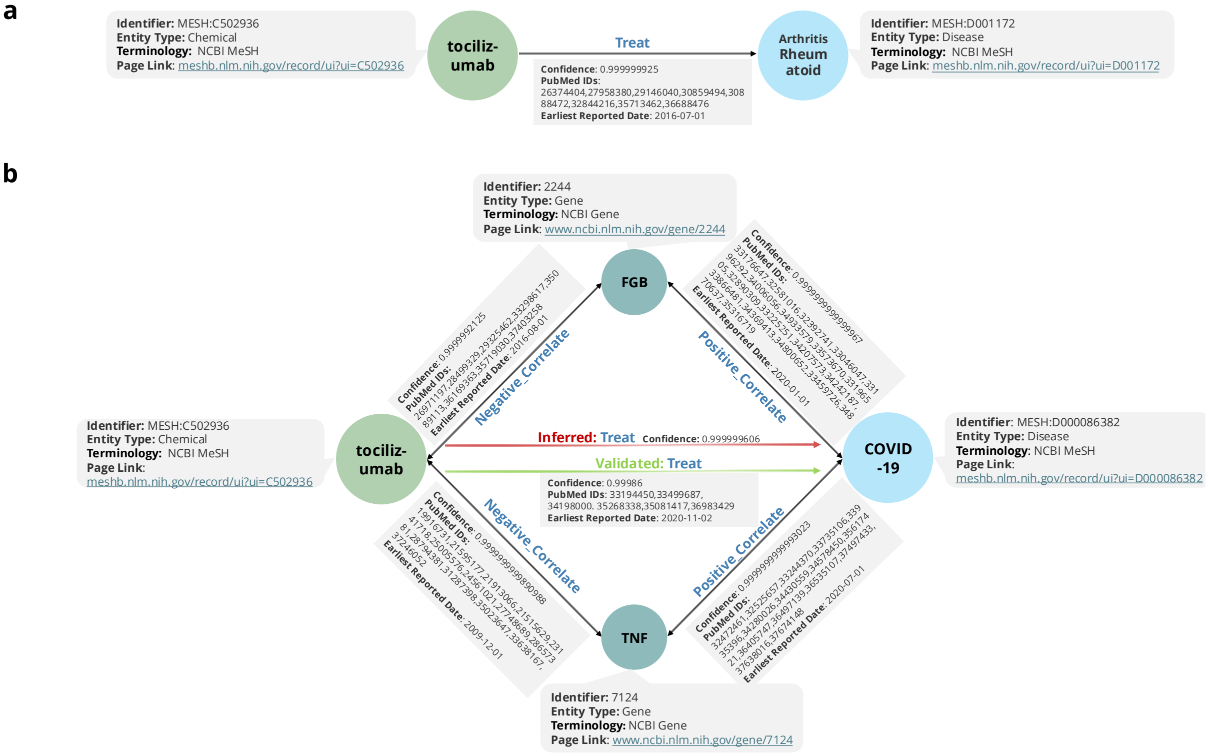
a
Identifier: MESH:C502936
Entity Type: Chemical
Terminology: NCBI MeSH
Page Link: meshb.nlm.nih.gov/record/ui?ui=C502936
tociliz-umab
Treat
Confidence: 0.999999925
PubMed IDs: 26374404,27958380,29146040,30859494,30888472,32844216,35713462,36688476
Earliest Reported Date: 2016-07-01
Arthritis Rheumatoid
Identifier: MESH:D001172
Entity Type: Disease
Terminology: NCBI MeSH
Page Link: meshb.nlm.nih.gov/record/ui?ui=D001172
b
Identifier: 2244
Entity Type: Gene
Terminology: NCBI Gene
Page Link: www.ncbi.nlm.nih.gov/gene/2244
FGB
Confidence: 0.9999992125
PubMed IDs: 26971197,28499329,29325462,33298617,35089113,36169363,35719030,37403258
Earliest Reported Date: 2016-08-01
Negative_Correlate
Confidence: 0.99999999999967
PubMed IDs: 33176647,32581016,32392741,33046047,33196292,34006056,34933579,33573670,33196505,32890309,33225251,34207573,34242187,33866481,34369413,34800652,33459726,34870637,35316719
Earliest Reported Date: 2020-01-01
Positive_Correlate
Identifier: MESH:C502936
Entity Type: Chemical
Terminology: NCBI MeSH
Page Link: meshb.nlm.nih.gov/record/ui?ui=C502936
tociliz-umab
Inferred: Treat Confidence: 0.999999606
Validated: Treat
Confidence: 0.99986
PubMed IDs: 33194450,33499687, 34198000. 35268338,35081417,36983429
Earliest Reported Date: 2020-11-02
COVID -19
Identifier: MESH:D000086382
Entity Type: Disease
Terminology: NCBI MeSH
Page Link: meshb.nlm.nih.gov/record/ui?ui=D000086382
Confidence: 0.99999999990988
PubMed IDs: 19916731,21595177,21913066,21515629,23141718,25005576,24561021,27748689,28657381,28794381,31287398,35023647,33638167,37246052
Earliest Reported Date: 2009-12-01
Negative_Correlate
Positive_Correlate
Confidence: 0.999999999993023
PubMed IDs: 32472461,32525657,33244370,33735106,33935396,34280026,34430559,34578450,35617421,36405747,36497139,36535107,37497433,37638016,37674148
Earliest Reported Date: 2020-07-01
TNF
Identifier: 7124
Entity Type: Gene
Terminology: NCBI Gene
Page Link: www.ncbi.nlm.nih.gov/gene/7124

Figure 5: Case study of tocilizumab for literature-based discovery and drug repurposing within the KG. **a**. Known association between tocilizumab and rheumatoid arthritis, supported by multiple publications, with the earliest reported date defined by the first extracted supporting paper. **b**. Two multi-hop reasoning paths linking tocilizumab to COVID-19 via intermediate genes FGB and TNF. The inferred *Treat* relation (red arrow) was derived solely from earlier literature, while later studies validated this prediction (green arrow). The temporal order of evidence highlights the KG's capacity to anticipate therapeutic connections prior to their recognition in the literature.

although lexically similar—exhibit greater internal consistency that may better align with the models' reasoning patterns. Together, these findings underscore the value of structured medical knowledge in enhancing the reasoning capacity and factual accuracy of leading LLMs across diverse clinical QA tasks.

2.5 Literature-Based Discovery and Drug Repurposing

To illustrate the capacity of the constructed KG to support literature-based discovery and drug repurposing, we examined the case of tocilizumab, a drug originally approved for the treatment of rheumatoid arthritis. Within the KG, this *Chemical–Disease* association is supported by multiple curated publications, as shown in Figure 5 **a**, which also highlights the earliest reported date of the relationship—defined as the publication date of the first source from which the association was extracted, based on the linked PubMed IDs.

To identify novel therapeutic hypotheses, we performed confidence-aware causal inference over *Chemical-Gene-Disease* pathways derived exclusively from preexisting literature. We focused on semantic patterns in which a chemical is negatively correlated with a gene that is positively correlated with a disease—suggesting that the chemical may exert a therapeutic effect by modulating the expression or activity of an intermediate gene involved in disease pathology. Applying the path pattern $\textit{Chemical} \xrightarrow{\textit{Negative\_Correlate}} \textit{Gene} \xrightarrow{\textit{Positive\_Correlate}} \textit{Disease}$, we fixed the chemical as tocilizumab and the disease as COVID-19. The reasoning module identified multiple plausible multi-hop pathways linking the two entities. Two representative examples are shown in Figure 5 **b**: (1) $\textit{tocilizumab} \xrightarrow{\textit{Negative\_Correlate}} \textit{FGB} \xrightarrow{\textit{Positive\_Correlate}} \textit{COVID-19}$ and (2) $\textit{tocilizumab} \xrightarrow{\textit{Negative\_Correlate}} \textit{TNF} \xrightarrow{\textit{Positive\_Correlate}} \textit{COVID-19}$. Both FGB and TNF are well-characterized mediators of inflammatory responses, reinforcing the biological plausibility of the inferred associations. Based on the causal inference framework and the identified paths, we formulated the $\textit{tocilizumab} \xrightarrow{\textit{Treat}} \textit{COVID-19}$ hypothesis (highlighted by the red arrow in Figure 5 **b**). The confidence score for this hypothesis was calculated as the average confidence across all supporting paths (using Equation (5)), with each path scored as the product of the confidence values of its constituent edges. These edge-level scores were derived from the frequency and consistency of co-mention evidence across earlier literature sources represented in the KG.

Importantly, this inference was generated using only literature published prior to the formal cognition of tocilizumab as a treatment for COVID-19. Subsequent studies have since provided independent evidence supporting its therapeutic efficacy (green arrow in Figure 5 **b**), thereby validating our earlier prediction, with a reported confidence level closely aligned with that of our inferred association. As shown in Figure 5 **b**, the earliest reported appearance of the tocilizumab–COVID-19 association occurred after the earliest appearances of each individual relationship along the causal inference path. This temporal precedence underscores the predictive power of the KG, which was able to anticipate therapeutically relevant links before they were explicitly acknowledged in the literature. Together, this case highlights the utility of KG-based reasoning in identifying previously unreported *Chemical-Disease* associations and guiding hypothesis-driven drug repositioning.

3 Discussion

The rapid growth and complexity of biomedical literature present significant challenges in organizing, synthesizing, and extracting actionable insights from vast amounts of unstructured text. Traditional methods for constructing biomedical KGs have struggled to keep pace with the evolving nature of scientific discovery, as they tend to treat literature as static, aggregating relational triples without accounting for temporal dynamics. In contrast, our work introduces MedKGent, a novel framework that constructs a temporally evolving medical KG, providing a more nuanced and adaptable solution for organizing biomedical knowledge.

MedKGent overcomes several key limitations of previous approaches by leveraging PubMed abstracts as its primary data source. PubMed provides a publicly accessible, large-scale, and continuously updated repository of biomedical literature that is well-structured and more amenable to LLM-based processing than real-world clinical data such as Electronic Health Records (EHRs), which are often fragmented, heterogeneous, and restricted by privacy concerns [84]. By processing PubMed abstracts incrementally on a daily basis, our framework preserves the chronological progression of medical knowledge, ensuring that the KG evolves alongside the development of the field. This dynamic method is essential for capturing the temporal nature of medical knowledge, where new findings often refine or challenge prior understanding. Moreover, this incremental processing enables the framework to seamlessly integrate future data, adapting effortlessly to new information as it emerges. The incorporation of confidence scores further enhances the system's ability to reinforce recurring knowledge and resolve conflicts, ensuring a more reliable and coherent representation of knowledge over time.

The results from our automated and expert evaluations indicate that MedKGent produces high-quality relational triples, with accuracy rates approaching 90%, and strong agreement across evaluators. This supports the framework's robustness and its ability to generate reliable biomedical knowledge at scale. Furthermore, the KG's integration with state-of-the-art LLMs in RAG tasks demonstrates its significant utility for clinical decision support and research. Notably, we observed consistent improvements in performance across a wide range of medical QA datasets, showcasing the KG's potential to enhance AI-driven solutions in healthcare.

Our approach also underscores the advantages of using LLMs for KG construction. Unlike traditional supervised methods that rely on fixed schemas and large volumes of annotated data, LLMs allow for greater generalizability and scalability in knowledge extraction. This generalizability is especially important in the medical domain, where new and emerging relations can be accommodated without requiring extensive retraining or re-annotation. The ability to extend the graph to include novel medical relations through prompt engineering further highlights the adaptability of MedKGent in dynamic medical environments.

One of the most compelling aspects of MedKGent is its application to drug repurposing. By leveraging the temporal and semantic richness of the constructed KG, we were able to uncover previously unreported chemical-disease treatment associations. These predictions, generated without access to future data, were later corroborated by independent publications, demonstrating the KG's predictive power and its potential to inform hypothesis-driven drug repositioning. This ability to identify emerging therapeutic connections has important implications for accelerating drug discovery, particularly in resource-limited settings where time and data are often constrained.

While MedKGent represents a substantial advancement over existing methods for KG construction, several challenges remain and present opportunities for future improvement. Although the framework dynamically integrates new knowledge, its performance remains dependent on the quality and completeness of the underlying literature. Expanding to incorporate additional sources—such as clinical trial registries or EHRs—could enhance both the comprehensiveness and clinical relevance of the resulting KG.

The flexible architecture of MedKGent also allows for adaptation to diverse data modalities and potential extension beyond the biomedical domain, supporting a wide range of applications. Nonetheless, a key limitation of

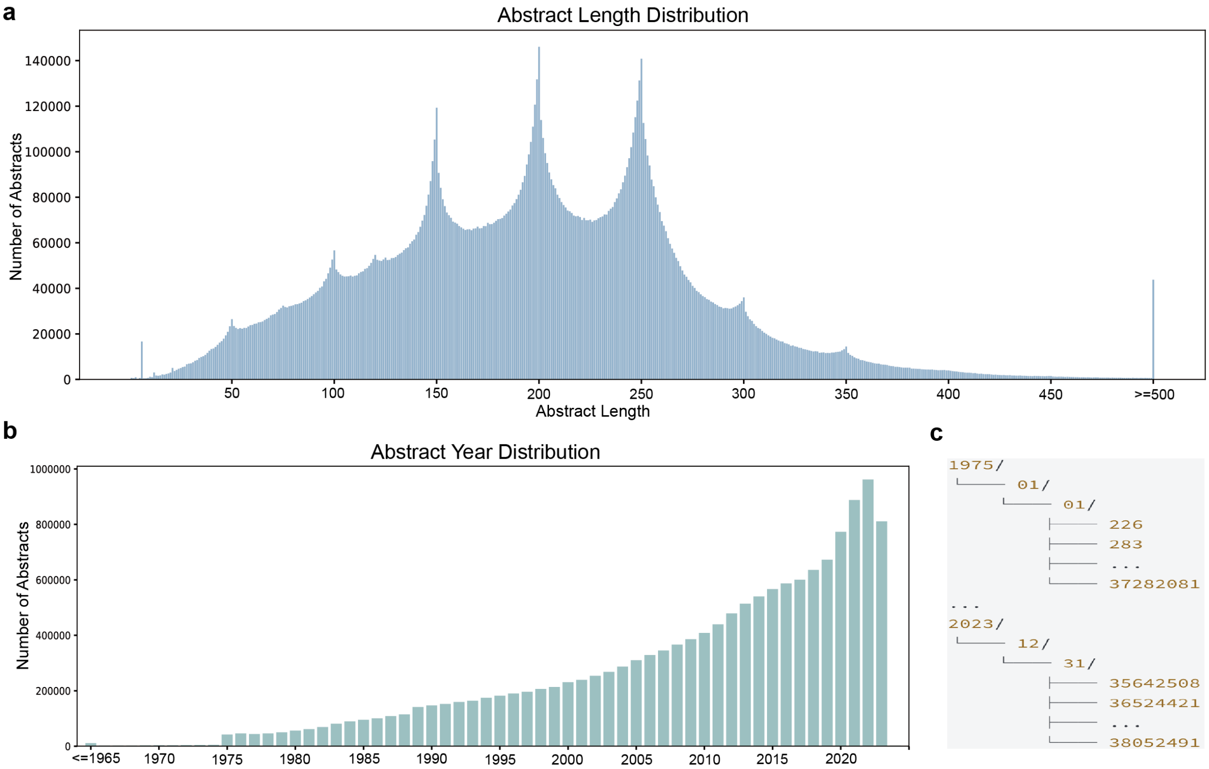

```
1975/
└── 01/
    └── 01/
        ├── 226
        ├── 283
        ├── ...
        └── 37282081
...
2023/
└── 12/
    └── 31/
        ├── 35642508
        ├── 36524421
        ├── ...
        └── 38052491
```

Extended Data Figure 1: Data preprocessing and curation of PubMed abstracts. Overview of the filtering and organization steps applied to over 20 million PubMed abstracts. Abstracts were filtered by length and publication year, and then structured into a daily time series from 1975 to 2023. **a**. Distribution of abstract lengths. The initial dataset displayed a long-tail distribution, with abstracts shorter than 100 words or longer than 500 words (aggregated for clarity) being infrequent and often containing uninformative content. Only abstracts ranging from 100 to 300 words were retained. **b**. Publication year distribution. A marked increase in publications began in 1975. Records from before 1965 were sparse and aggregated, while data from 2024 were excluded due to incompleteness. The final dataset spans 1975-2023. **c**. Daily time series structure. A total of 10,014,314 abstracts were organized into a fine-grained daily time series from January 1, 1975, to December 31, 2023. Abstracts published on the same day were ordered by ascending PubMed ID to ensure intra-day consistency.

LLM-based knowledge extraction is the risk of "hallucination", in which models generate plausible but factually incorrect information. In addition, LLMs may struggle to reflect the most recent scientific developments due to fixed training cutoffs. MedKGent's model-agnostic design enables seamless replacement of its underlying LLM with more advanced or updated models, ensuring ongoing improvements in both knowledge extraction and integration. Future work may also focus on refining the confidence scoring mechanism. More sophisticated techniques—such as Bayesian modeling or explicit uncertainty quantification—could yield finer-grained estimates of triple reliability. Such enhancements may improve interpretability and support more transparent, trustworthy decision-making in clinical contexts.

In conclusion, MedKGent marks a significant advancement in the automatic construction of medical KGs, providing a scalable, flexible, and reliable framework for organizing and leveraging biomedical knowledge. Its capacity to capture the dynamic nature of scientific discovery, combined with its robust performance in clinical applications, establishes it as a valuable tool for advancing medical research, clinical decision support, and AI-driven drug discovery. Future developments are expected to broaden its scope, refine its algorithms, and further enhance its ability to deliver real-time, data-driven insights in medicine.

4 Methods

4.1 Data Preprocessing

We selected PubMed abstracts as the primary data source for constructing the medical KG, owing to their concise yet information-dense summaries of research findings. The structured format and compact content of these abstracts make them particularly suitable for large-scale knowledge extraction. Over 20 million abstracts were collected from the PubMed[3], which integrates biomedical literature with specific publication dates. After excluding entries that failed to download or lacked abstract content—commonly due to missing metadata in older records—we retained more than 16 million abstracts for further analysis.

We first analyzed the length distribution of the abstracts (Extended Data Figure 1 **a**), which followed a characteristic long-tail pattern. A small proportion of abstracts exceeded 500 words; for clarity, all abstracts longer than 500 words were aggregated into a single group, while a considerable number were shorter than 100 words. Manual inspection indicated that both extremes often contained irregular or uninformative content. To improve consistency and reduce noise, we retained only abstracts within the 100–300 word range, the most common length observed. Next, We analyzed the distribution of publication years (Extended Data Figure 1 **b**). Articles published before 1965 were rare and were aggregated for reference. A notable increase in publication volume began in 1975, while records from 2024 were incomplete at the time of data collection. As a result, we restricted our dataset to abstracts published between 1975 and 2023. Following a series of quality control procedures—including length filtering, temporal constraints, and content-based screening—we retained a total of 10,014,314 PubMed abstracts. These abstracts were organized into a fine-grained daily time series from January 1, 1975, to December 31, 2023 (Extended Data Figure 1 **c**), facilitating high-resolution temporal analysis of the emergence of medical knowledge. To ensure intra-day consistency, abstracts published on the same date were sorted by ascending PubMed ID.

4.2 MedKGent Framework

We developed MedKGent, a LLM-based agent framework for constructing a temporally evolving medical KG. MedKGent processes biomedical abstracts sequentially from January 1, 1975, to December 31, 2023, allowing the KG to grow incrementally in step with the historical development of medical knowledge while remaining extensible to future updates. The framework comprises two coordinated agents—the Extractor Agent and the Constructor Agent—deployed via a self-hosted API based on the open-source Qwen2.5-32B-Instruct model [70]. Deployment leveraged 48 NVIDIA L20Z GPUs (80 GB each), with two services per GPU, totaling 96 services. This setup significantly reduces costs compared to commercial LLM APIs, particularly given the large volume of abstracts processed, and provides greater flexibility for system optimization, including improved message queue throughput and processing speed. Collectively, the two agents extract structured medical facts and integrate them into a dynamic, time-aware KG.

4.2.1 Extractor Agent

The Extractor Agent identifies biomedical entities within each abstract using PubTator3 [80], an off-the-shelf AI tool developed and continuously maintained by the NCBI. This module annotates six categories of biomedical entities—genes, diseases, chemicals, variants, species, and cell lines—producing an entity set $E = \{e_1, e_2, \cdots\}$ extracted from a given abstract A. While LLMs can jointly extract entities and relational triples via prompting, the Extractor Agent adopts a decoupled strategy: entities are first annotated using PubTator3 tool, followed by relation extraction with the LLM. This design offers several key advantages. First, PubTator3 tool not only detects biomedical concepts but also assigns unique identifiers, normalizing synonymous mentions to standardized terminology entries. These identifiers facilitate downstream tasks such as entity disambiguation, merging, and retrieval—critical steps for accurate graph construction by the Constructor Agent. The terminologies used for each entity type are summarized in Extended Data Figure 2 **b**. Second, PubTator3 tool provides state-of-the-art entity annotations across PubMed abstracts and is widely adopted within the biomedical research community. Third, decoupling the tasks allows the LLM to focus exclusively on relation extraction, reducing cognitive load and enhancing overall performance relative to joint extraction approaches.

Given both the abstract A and its extracted entity set E, the Extractor Agent then prompts the LLM to infer semantic relationships between entity pairs, guided by a predefined set of relation types R and their textual definitions. Leveraging the LLM's internal knowledge, it assigns a relation $r_n \in R$ to each relevant entity pair $(e_i, e_j) \in E$, resulting in a set of candidate relational triples $T_{\text{candi}} = \{t_1, t_2, \cdots | t_k = (e_i, r_n, e_j)\}$. The prompting

[3] https://pubmed.ncbi.nlm.nih.gov/

template used for this inference is illustrated in Extended Data Figure 2 **a**. We define a set of 12 core biomedical relation types, comprising seven bidirectional relations—Associate, Negative_Correlate, Positive_Correlate, Compare, Cotreat, Interact, and Drug_Interact—and five unidirectional relations—Cause, Inhibit, Treat, Stimulate, and Prevent. The properties and descriptions of these relations are detailed in Extended Data Figure 2 **d**. These relation types can be flexibly extended through prompt design as needed. This adaptable design eliminates the need for rigid schema definitions or retraining, as required in traditional supervised pipelines, allowing MedKGent to incorporate novel and evolving medical relations with minimal manual intervention.

To assign an initial confidence score to each extracted relational triple, the Extractor Agent employs a sampling-based confidence estimation strategy during LLM inference, inspired by the self-consistency principle [71–73,85]. Specifically, for a extraction prompt, the agent performs N parallel inferences (with $N = 50$), yielding N sets of candidate triples, denoted as $\{T^1_{\text{candi}}, \cdots, T^N_{\text{candi}}\}$, each corresponding to a separate inference. To enhance output diversity, the LLM within the Extractor Agent operates with an elevated temperature coefficient ($\tau = 0.7$), increasing the randomness of its predictions. This adjustment fosters variability across the generated triples, thereby improving the robustness of the extraction process. Following this, the Extractor Agent conducts a formatting check on all candidate triples, eliminating those containing extraneous or irrelevant characters. For the remaining triples, the agent computes initial confidence scores based on their frequency of occurrence across the N inference runs. Each frequency is normalized by mapping it to the nearest lower multiple of 0.05, which is then assigned as the triple's initial confidence score. This process reflects the consistency of the model's predictions while ensuring that the confidence scores are appropriately scaled.

Following the assignment of initial confidence scores, the Extractor Agent filters out low-confidence relational triples (score < 0.6), retaining only high-confidence triples for downstream graph construction. For each retained triple, the agent enriches both head and tail entities with two key attributes—Exact Keywords and Semantic Embedding—in addition to the original name, entity type, unique identifier, and terminology. Exact Keywords list all textual variants of the entity within the abstract (standardized to lowercase and mapped to a single identifier), while Semantic Embedding represents the entity as a 768-dimensional vector generated using the BiomedNLP-BiomedBERT-base-uncased-abstract-fulltext model [81]. These enriched representations improve the precision and efficiency of information retrieval in downstream clinical applications, particularly when explicit entity identifiers are unavailable. Each triple is further annotated with the PubMed ID of the source abstract and a timestamp corresponding to the publication date, ensuring full traceability and source attribution. The final set of enriched triples is then passed to the Constructor Agent for integration into the KG.

4.2.2 Constructor Agent

The Constructor Agent incrementally integrates relational triples extracted by the Extractor Agent into a dynamically evolving temporal KG through continuous interaction with a Neo4j graph database.

For each relational triple, the Constructor Agent first checks whether the head and tail entities—identified by their unique identifiers—already exist in the graph. If either entity is absent, the corresponding node is inserted, and a new edge is created to represent the specified relationship. If both entities are present and the relation type matches that of an existing edge, the triple is interpreted as a recurrence of the same medical knowledge in a subsequent publication. In this case, the graph is updated by increasing the edge's confidence score s using the following enhancement function:

$$s = 1 - (1 - s) * (1 - s'), \tag{1}$$

where s' is the confidence score of the newly observed triple. This formulation ensures that confidence increases monotonically as evidence accumulates; the more frequently the same knowledge appears during graph construction, the higher its resulting confidence. The PubMed ID associated with the new occurrence is appended to the edge's PubMed ID list of supporting references, and the Timestamp is updated to reflect the most recent publication. Historical provenance is preserved through the complete PubMed ID list, enabling full traceability of supporting evidence over time. Conversely, if both entities exist but the relation type differs from that of the existing edge, this suggests that multiple relationships have been assigned to the same entity pair. To avoid redundancy and inconsistency, we assume that only one, most appropriate relation should be maintained. In such cases, the Constructor Agent invokes a LLM to resolve the conflict by selecting the more suitable relation, considering the confidence score s and timestamp t of the existing edge, as well as the confidence score s' and timestamp t' of the incoming triple. To ensure more deterministic output than that used in the Extractor Agent, the LLM in the Constructor Agent is configured with a lower temperature parameter ($\tau = 0.2$). The prompting strategy for this decision process is illustrated in Extended Data Figure 2 **c**.

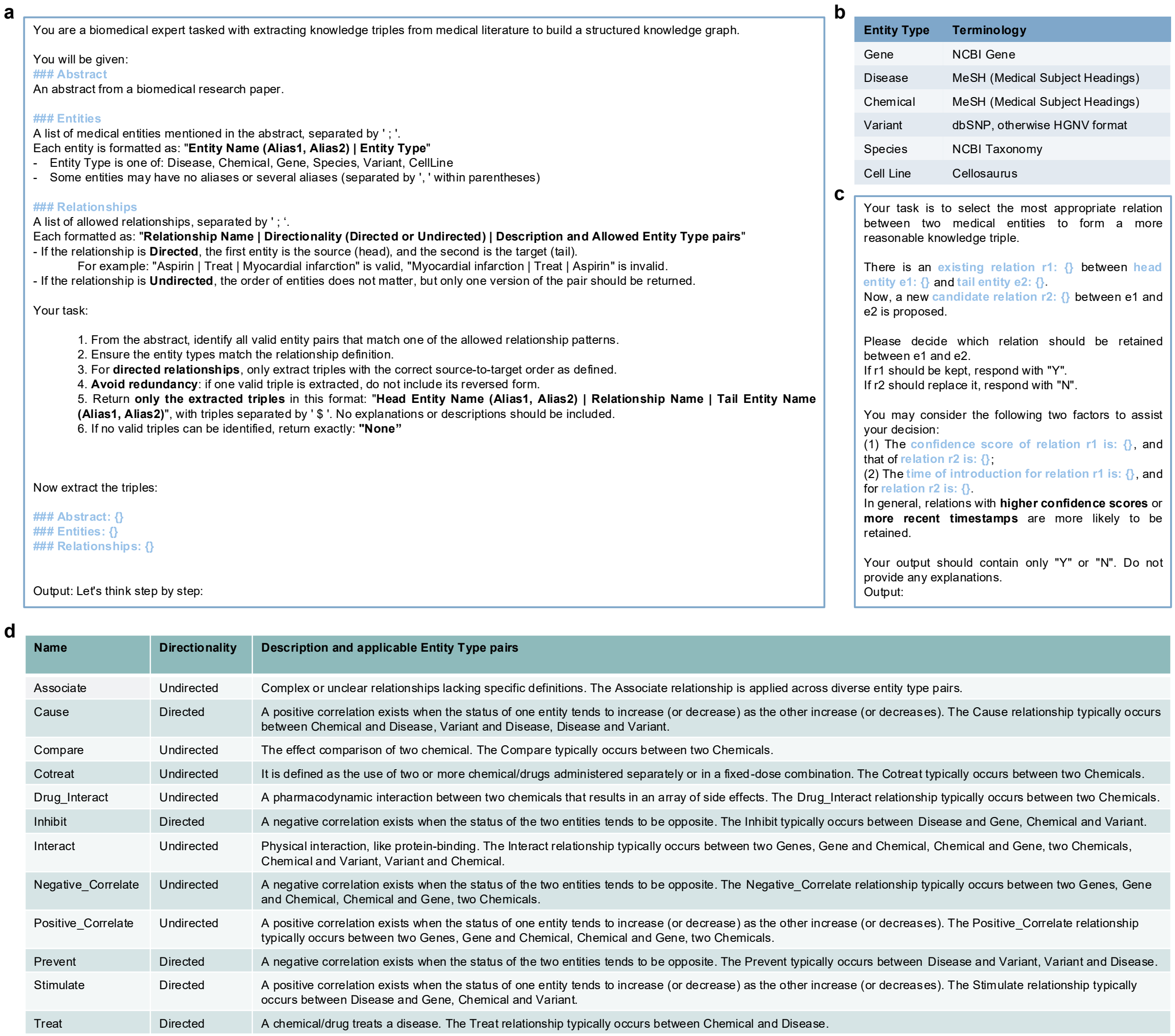

a

You are a biomedical expert tasked with extracting knowledge triples from medical literature to build a structured knowledge graph.

You will be given:
Abstract
An abstract from a biomedical research paper.

Entities
A list of medical entities mentioned in the abstract, separated by ' ; '.
Each entity is formatted as: "**Entity Name (Alias1, Alias2) | Entity Type**"
- Entity Type is one of: Disease, Chemical, Gene, Species, Variant, CellLine
- Some entities may have no aliases or several aliases (separated by ', ' within parentheses)

Relationships
A list of allowed relationships, separated by ' ; '.
Each formatted as: "**Relationship Name | Directionality (Directed or Undirected) | Description and Allowed Entity Type pairs**"
- If the relationship is **Directed**, the first entity is the source (head), and the second is the target (tail).
For example: "Aspirin | Treat | Myocardial infarction" is valid, "Myocardial infarction | Treat | Aspirin" is invalid.
- If the relationship is **Undirected**, the order of entities does not matter, but only one version of the pair should be returned.

Your task:

1. From the abstract, identify all valid entity pairs that match one of the allowed relationship patterns.
2. Ensure the entity types match the relationship definition.
3. For **directed relationships**, only extract triples with the correct source-to-target order as defined.
4. **Avoid redundancy**: if one valid triple is extracted, do not include its reversed form.
5. Return **only the extracted triples** in this format: "**Head Entity Name (Alias1, Alias2) | Relationship Name | Tail Entity Name (Alias1, Alias2)**", with triples separated by ' $ '. No explanations or descriptions should be included.
6. If no valid triples can be identified, return exactly: **"None"**

Now extract the triples:

Abstract: {}
Entities: {}
Relationships: {}

Output: Let's think step by step:

b

Entity Type	Terminology
Gene	NCBI Gene
Disease	MeSH (Medical Subject Headings)
Chemical	MeSH (Medical Subject Headings)
Variant	dbSNP, otherwise HGNV format
Species	NCBI Taxonomy
Cell Line	Cellosaurus

c

Your task is to select the most appropriate relation between two medical entities to form a more reasonable knowledge triple.

There is an existing relation r1: {} between head entity e1: {} and tail entity e2: {}.
Now, a new candidate relation r2: {} between e1 and e2 is proposed.

Please decide which relation should be retained between e1 and e2.
If r1 should be kept, respond with "Y".
If r2 should replace it, respond with "N".

You may consider the following two factors to assist your decision:
(1) The confidence score of relation r1 is: {}, and that of relation r2 is: {};
(2) The time of introduction for relation r1 is: {}, and for relation r2 is: {}.
In general, relations with **higher confidence scores** or **more recent timestamps** are more likely to be retained.

Your output should contain only "Y" or "N". Do not provide any explanations.
Output:

d

Name	Directionality	Description and applicable Entity Type pairs
Associate	Undirected	Complex or unclear relationships lacking specific definitions. The Associate relationship is applied across diverse entity type pairs.
Cause	Directed	A positive correlation exists when the status of one entity tends to increase (or decrease) as the other increase (or decreases). The Cause relationship typically occurs between Chemical and Disease, Variant and Disease, Disease and Variant.
Compare	Undirected	The effect comparison of two chemical. The Compare typically occurs between two Chemicals.
Cotreat	Undirected	It is defined as the use of two or more chemical/drugs administered separately or in a fixed-dose combination. The Cotreat typically occurs between two Chemicals.
Drug_Interact	Undirected	A pharmacodynamic interaction between two chemicals that results in an array of side effects. The Drug_Interact relationship typically occurs between two Chemicals.
Inhibit	Directed	A negative correlation exists when the status of the two entities tends to be opposite. The Inhibit typically occurs between Disease and Gene, Chemical and Variant.
Interact	Undirected	Physical interaction, like protein-binding. The Interact relationship typically occurs between two Genes, Gene and Chemical, Chemical and Gene, two Chemicals, Chemical and Variant, Variant and Chemical.
Negative_Correlate	Undirected	A negative correlation exists when the status of the two entities tends to be opposite. The Negative_Correlate relationship typically occurs between two Genes, Gene and Chemical, Chemical and Gene, two Chemicals.
Positive_Correlate	Undirected	A positive correlation exists when the status of one entity tends to increase (or decrease) as the other increase (or decreases). The Positive_Correlate relationship typically occurs between two Genes, Gene and Chemical, Chemical and Gene, two Chemicals.
Prevent	Directed	A negative correlation exists when the status of the two entities tends to be opposite. The Prevent typically occurs between Disease and Variant, Variant and Disease.
Stimulate	Directed	A positive correlation exists when the status of one entity tends to increase (or decrease) as the other increase (or decreases). The Stimulate relationship typically occurs between Disease and Gene, Chemical and Variant.
Treat	Directed	A chemical/drug treats a disease. The Treat relationship typically occurs between Chemical and Disease.

Extended Data Figure 2: **a**. Prompt template for relation extraction. Given a biomedical abstract and its extracted entities, the Extractor Agent prompts the LLM to infer semantic relations between entity pairs using a predefined relation set and textual descriptions. **b**. Reference terminologies for entity normalization. Each biomedical entity type is mapped to a standard terminology: Gene (NCBI Gene), Disease and Chemical (MeSH), Variant (dbSNP or HGNV), Species (NCBI Taxonomy), and Cell Line (Cellosaurus). **c**. Prompt design for relation conflict resolution. When conflicting relations exist between the same entity pair, the Constructor Agent prompts the LLM to select the most appropriate one based on confidence scores and timestamps. **d**. Schema for predefined relation types. The 12 core relation types—seven bidirectional and five unidirectional—are listed alongside their directionality, descriptions, and allowed entity-type combinations.

4.3 Quality Assessment

We assessed the quality of relational triples extracted by the Extractor Agent through both automated and manual evaluations, leveraging two state-of-the-art LLMs—GPT-4.1 [74] and DeepSeek-v3 [75]—as well as three PhD students with interdisciplinary expertise in medicine and computer science. For each medical abstract and its corresponding set of extracted triples, individual triples were evaluated using a standardized four-level scoring rubric: 3.0 (Correct), 2.0 (Likely Correct), 1.0 (Likely Incorrect), and 0.0 (Incorrect). The evaluation prompt provided to both LLMs and human annotators is illustrated in Extended Data Figure 3 **a**.

A relational triple was defined as *valid* if it received a score of ≥ 2.0. The validity rate was calculated as:

$$Validity\ Rate = \frac{Number\ of\ triples\ with\ score \geq 2.0}{Total\ number\ of\ evaluated\ triples}. \tag{2}$$

To assess the reliability of automatic evaluation, we compared LLM-based assessments with human annotations on a shared evaluation subset, treating human judgments as ground truth. The precision, recall, and F_1-score of the automatic evaluations were computed as:

$$Precision = \frac{TP}{TP + FP},\ Recall = \frac{TP}{TP + FN},\ F_1 = \frac{2 \times Precision \times Recall}{Precision + Recall}, \tag{3}$$

where TP, FP, and FN represent true positives, false positives, and false negatives, respectively. To further quantify inter-rater agreement, we calculated Cohen's Kappa coefficient [82] for each pair of evaluators, including both LLMs and human annotators, resulting in 10 pairwise comparisons across the five raters. The Kappa coefficient was computed as:

$$\kappa = \frac{p_0 - p_e}{1 - p_e}, \tag{4}$$

where p_0 represents the observed agreement and p_e denotes the expected agreement by chance. This analysis provides a quantitative measure of rating consistency across evaluators.

4.4 Retrieval-Augmented Generation

The constructed KG serves as a reliable external source for information retrieval and can be integrated into LLMs via a RAG framework. By providing structured biomedical context, the KG enhances LLM performance across a range of medical QA benchmarks.

Given a user query q, we first extract the set of medical entities present in the question, denoted as $E^q = \{e_1^q, e_2^q, \cdots\}$. When using PubTator3 [80]—the same entity recognition tool employed during KG construction—each extracted entity is assigned a unique identifier. This allows for efficient entity linking by matching these identifiers to the corresponding nodes $N^q = \{n_1^q, n_2^q, \cdots\}$ within the graph. Alternatively, if medical entities are extracted using other methods—such as prompting a LLM—they may lack standardized identifiers. In such cases, the extracted entity mentions are first converted to lowercase and matched against the Exact Keywords attribute of each node in the KG. A successful match enables linkage of the entity to the corresponding graph node. In both approaches, if an entity cannot be linked via its identifier or if its surface form does not appear in any node's Exact Keywords list, we apply a semantic similarity strategy to complete the entity linking process. Specifically, the embedding of the query entity is computed using the same model employed for generating node-level semantic representations (*i.e.*, BiomedNLP-BiomedBERT-base-uncased-abstract-fulltext [81]) and is compared against the Semantic Embedding of all nodes in the KG. The entity is then linked to the node with the highest semantic similarity score, which may correspond to either the exact concept or a semantically related medical entity. This entity linking framework—combining identifier-based matching, lexical normalization, and semantic embedding—ensures robust and flexible integration of KG-derived knowledge into downstream QA tasks.

Following entity linking, we construct evidence subgraphs using a neighbor-based exploration strategy [86] to enhance the reasoning capabilities of LLMs. For each entity-linked node in the query-specific set N^q, we retrieve its one-hop neighbors within the KG. Specifically, for each node $n_i^q \in N^q$, all adjacent nodes $n_i^{q'}$ are identified, and the corresponding triples $(n_i^q, r, n_i^{q'})$ are appended to form a localized subgraph G_i^q. This expansion captures the immediate relational context surrounding the query entities, which is essential for enabling fine-grained medical reasoning. The complete evidence set for a given query is then defined as the union of these localized subgraphs: $G^q = \{G_1^q, G_2^q, \cdots\}$. The resulting subgraph G^q may contain a large number of relational triples, including redundant or irrelevant information, which can adversely impact LLM reasoning [87]. To address this, we leverage the LLM's inherent ranking capability to selectively filter high-value knowledge [88]. Given the question q and

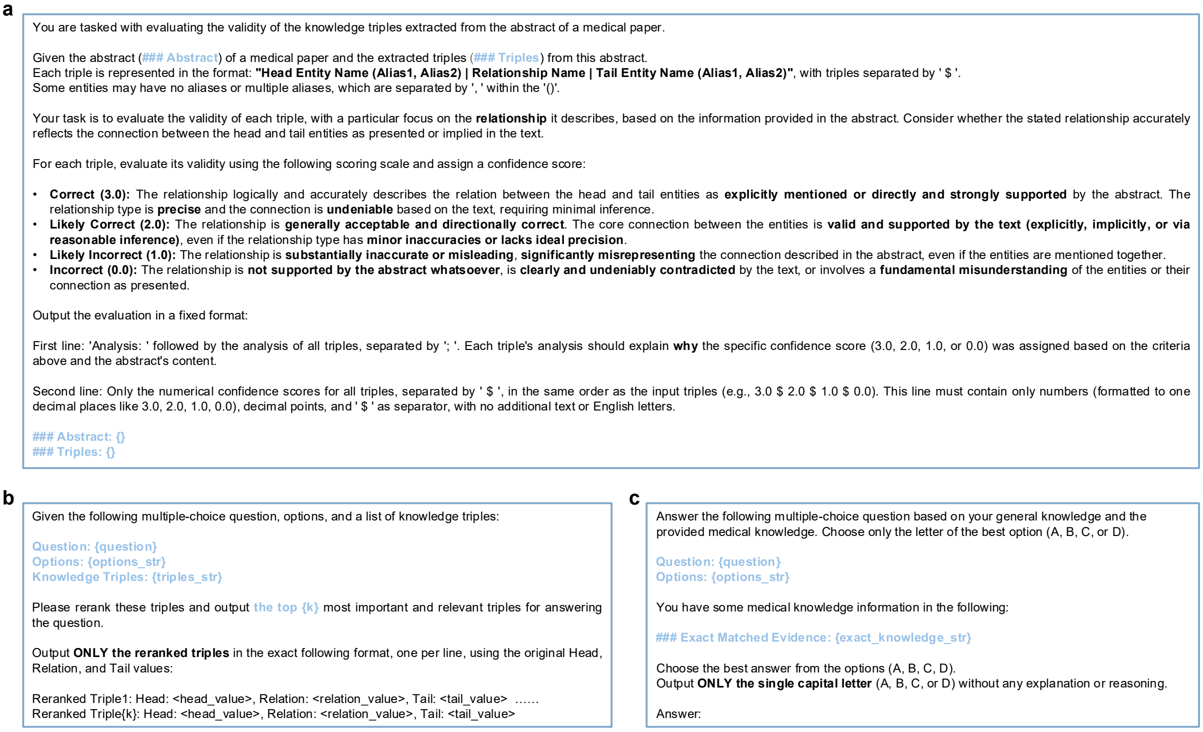

You are tasked with evaluating the validity of the knowledge triples extracted from the abstract of a medical paper.

Given the abstract (### Abstract) of a medical paper and the extracted triples (### Triples) from this abstract.
Each triple is represented in the format: **"Head Entity Name (Alias1, Alias2) | Relationship Name | Tail Entity Name (Alias1, Alias2)"**, with triples separated by ' $ '.
Some entities may have no aliases or multiple aliases, which are separated by ', ' within the '()'.

Your task is to evaluate the validity of each triple, with a particular focus on the **relationship** it describes, based on the information provided in the abstract. Consider whether the stated relationship accurately reflects the connection between the head and tail entities as presented or implied in the text.

For each triple, evaluate its validity using the following scoring scale and assign a confidence score:

- **Correct (3.0):** The relationship logically and accurately describes the relation between the head and tail entities as **explicitly mentioned or directly and strongly supported** by the abstract. The relationship type is **precise** and the connection is **undeniable** based on the text, requiring minimal inference.
- **Likely Correct (2.0):** The relationship is **generally acceptable and directionally correct**. The core connection between the entities is **valid and supported by the text (explicitly, implicitly, or via reasonable inference)**, even if the relationship type has **minor inaccuracies or lacks ideal precision**.
- **Likely Incorrect (1.0):** The relationship is **substantially inaccurate or misleading**, **significantly misrepresenting** the connection described in the abstract, even if the entities are mentioned together.
- **Incorrect (0.0):** The relationship is **not supported by the abstract whatsoever**, is **clearly and undeniably contradicted** by the text, or involves a **fundamental misunderstanding** of the entities or their connection as presented.

Output the evaluation in a fixed format:

First line: 'Analysis: ' followed by the analysis of all triples, separated by '; '. Each triple's analysis should explain **why** the specific confidence score (3.0, 2.0, 1.0, or 0.0) was assigned based on the criteria above and the abstract's content.

Second line: Only the numerical confidence scores for all triples, separated by ' $ ', in the same order as the input triples (e.g., 3.0 $ 2.0 $ 1.0 $ 0.0). This line must contain only numbers (formatted to one decimal places like 3.0, 2.0, 1.0, 0.0), decimal points, and ' $ ' as separator, with no additional text or English letters.

### Abstract: {}
### Triples: {}

Given the following multiple-choice question, options, and a list of knowledge triples:

Question: {question}
Options: {options_str}
Knowledge Triples: {triples_str}

Please rerank these triples and output the top {k} most important and relevant triples for answering the question.

Output **ONLY the reranked triples** in the exact following format, one per line, using the original Head, Relation, and Tail values:

Reranked Triple1: Head: <head_value>, Relation: <relation_value>, Tail: <tail_value> ……
Reranked Triple{k}: Head: <head_value>, Relation: <relation_value>, Tail: <tail_value>

Answer the following multiple-choice question based on your general knowledge and the provided medical knowledge. Choose only the letter of the best option (A, B, C, or D).

Question: {question}
Options: {options_str}

You have some medical knowledge information in the following:

### Exact Matched Evidence: {exact_knowledge_str}

Choose the best answer from the options (A, B, C, D).
Output **ONLY the single capital letter** (A, B, C, or D) without any explanation or reasoning.

Answer:

Extended Data Figure 3: **a**. Prompt used for manual and LLM-based triple quality evaluation. A standardized prompt presenting extracted relational triples was used to guide assessments by LLMs and domain-trained human annotators. Each triple was scored on a four-level rubric ranging from 0.0 (Incorrect) to 3.0 (Correct). **b**. Prompt for subgraph reranking based on query relevance. Given a query and its associated knowledge subgraph, the LLM is prompted to rank triples by their relevance to the question. The top-k triples are retained to construct a refined subgraph used for downstream reasoning. **c**. Prompt for final answer generation. In the reasoning phase, the question and the reranked subgraph are provided to the LLM to generate an answer. This focused context reduces cognitive noise and improves response quality.

its corresponding subgraph G^q, we prompt the LLM to rerank the triples based on their relevance to the query. Only the top k triples ($k = 5$) are retained to form a refined subgraph G^q_{rerank}. The reranking prompt is shown in Extended Data Figure 3 **b**. In the final reasoning stage, the question q and the refined subgraph G^q_{rerank} are provided to the LLM for answer generation. This targeted context significantly reduces cognitive noise and improves answer quality. The final inference prompt is illustrated in Extended Data Figure 3 **c**.

4.5 Literature-Based Drug Repurposing

To evaluate the potential of the constructed KG to support literature-based drug repurposing, we performed confidence-aware causal inference over *Chemical-Gene-Disease* pathways derived exclusively from earlier literature snapshots. By leveraging the KG's heterogeneous structure, semantically enriched relationships, and temporal annotations, we aimed to identify previously unreported *Chemical–Disease* treatment associations.

We focused on two-hop semantic paths of the form $Chemical \xrightarrow{r_1} Gene \xrightarrow{r_2} Disease$, where ($r_1$, r_2) corresponds to the relation pair (Negative_Correlate, Positive_Correlate). The underlying rationale is that a chemical negatively correlated with a gene, whose expression is positively correlated with a disease, may exert a therapeutic effect by modulating that gene's role in disease pathophysiology. The inverse configuration (Positive_Correlate, Negative_Correlate) also applies, but the approach is illustrated using the (Negative_Correlate, Positive_Correlate) schema. For instance, when instantiating a chemical such as tocilizumab and a disease such as COVID-19, we queried the KG for supporting paths that conformed to the defined semantic pattern. The analysis revealed multiple plausible pathways of the form $tocilizumab \xrightarrow{Negative\_Correlate} Gene \xrightarrow{Positive\_Correlate} COVID$-19, involving several distinct intermediate gene nodes. These findings suggested a potential treatment association between tocilizumab and COVID-19. Notably, this inference was later corroborated by independent studies in subsequent publications, underscoring the KG's ability to anticipate emerging therapeutic relationships.

To assign a confidence score to each inferred treatment association, we aggregated information across all supporting paths. The confidence score for a candidate $Chemical \xrightarrow{Treat} Disease$ relation was computed as the average path confidence, where each path was scored as the product of the confidence values of its constituent edges. Formally, let P denote the set of all valid paths connecting a chemical c to a disease d. The overall confidence score $S(c, d)$ is defined as:

$$S(c,d) = \frac{1}{|P|} \sum_{p \in P} \prod_{(e_i, r, e_j) \in p} s(e_i, r, e_j), \tag{5}$$

where $s(e_i, r, e_j)$ denotes the confidence score of edge/triple (e_i, r, e_j) along path p.

This approach demonstrates the KG's utility not only as a structured repository of biomedical knowledge but also as a predictive engine for hypothesis generation and data-driven therapeutic discovery.

5 Data availability

The medical knowledge graph constructed in this study is publicly available at https://huggingface.co/datasets/ShowerMaker/MedKGent-KG.

6 Code availability

The source code for MedKGent will be available at https://github.com/BladeDancer957/MedKGent.

References

[1] Adanma Cecilia Eberendu et al. Unstructured Data: an overview of the data of Big Data. *International Journal of Computer Trends and Technology*, 38(1):46–50, 2016.

[2] Qiao Jin, Robert Leaman, and Zhiyong Lu. PubMed and beyond: biomedical literature search in the age of artificial intelligence. *EBioMedicine*, 100, 2024.

[3] Ling Wang, Haoyu Hao, Xue Yan, Tie Hua Zhou, and Keun Ho Ryu. From biomedical knowledge graph construction to semantic querying: a comprehensive approach. *Scientific Reports*, 15(1):8523, 2025.

[4] Wasim Aftab, Zivkos Apostolou, Karim Bouazoune, and Tobias Straub. Optimizing biomedical information retrieval with a keyword frequency-driven prompt enhancement strategy. *BMC bioinformatics*, 25(1):281, 2024.

[5] Linfeng Li, Peng Wang, Jun Yan, Yao Wang, Simin Li, Jinpeng Jiang, Zhe Sun, Buzhou Tang, Tsung-Hui Chang, Shenghui Wang, et al. Real-world data medical knowledge graph: construction and applications. *Artificial intelligence in medicine*, 103:101817, 2020.

[6] Sheng Yu, Zheng Yuan, Jun Xia, Shengxuan Luo, Huaiyuan Ying, Sihang Zeng, Jingyi Ren, Hongyi Yuan, Zhengyun Zhao, Yucong Lin, et al. Bios: An algorithmically generated biomedical knowledge graph. *arXiv preprint arXiv:2203.09975*, 2022.

[7] Xiaojun Chen, Shengbin Jia, and Yang Xiang. A review: Knowledge reasoning over knowledge graph. *Expert systems with applications*, 141:112948, 2020.

[8] Aidan Hogan, Eva Blomqvist, Michael Cochez, Claudia d'Amato, Gerard De Melo, Claudio Gutierrez, Sabrina Kirrane, José Emilio Labra Gayo, Roberto Navigli, Sebastian Neumaier, et al. Knowledge graphs. *ACM Computing Surveys (Csur)*, 54(4):1–37, 2021.

[9] David N Nicholson and Casey S Greene. Constructing knowledge graphs and their biomedical applications. *Computational and structural biotechnology journal*, 18:1414–1428, 2020.

[10] Zhenxiang Gao, Pingjian Ding, and Rong Xu. KG-Predict: A knowledge graph computational framework for drug repurposing. *Journal of biomedical informatics*, 132:104133, 2022.

[11] Shuangjia Zheng, Jiahua Rao, Ying Song, Jixian Zhang, Xianglu Xiao, Evandro Fei Fang, Yuedong Yang, and Zhangming Niu. PharmKG: a dedicated knowledge graph benchmark for bomedical data mining. *Briefings in bioinformatics*, 22(4):bbaa344, 2021.

[12] Jiageng Wu, Xian Wu, and Jie Yang. Guiding clinical reasoning with large language models via knowledge seeds. In *Proceedings of the Thirty-Third International Joint Conference on Artificial Intelligence*, pages 7491–7499, 2024.

[13] Nan Li, Zhihao Yang, Ling Luo, Lei Wang, Yin Zhang, Hongfei Lin, and Jian Wang. KGHC: a knowledge graph for hepatocellular carcinoma. *BMC Medical Informatics and Decision Making*, 20:1–11, 2020.

[14] Patrick Ernst, Amy Siu, and Gerhard Weikum. Knowlife: a versatile approach for constructing a large knowledge graph for biomedical sciences. *BMC bioinformatics*, 16:1–13, 2015.

[15] Zara Nasar, Syed Waqar Jaffry, and Muhammad Kamran Malik. Named entity recognition and relation extraction: State-of-the-art. *ACM Computing Surveys (CSUR)*, 54(1):1–39, 2021.

[16] Sonit Singh. Natural language processing for information extraction. *arXiv preprint arXiv:1807.02383*, 2018.

[17] Georgios Petasis, Frantz Vichot, Francis Wolinski, Georgios Paliouras, Vangelis Karkaletsis, and Constantine D Spyropoulos. Using machine learning to maintain rule-based named-entity recognition and classification systems. In *proceedings of the 39th annual meeting of the association for computational linguistics*, pages 426–433, 2001.

[18] Ji-Hwan Kim and Philip C Woodland. A rule-based named entity recognition system for speech input. In *INTERSPEECH*, pages 528–531, 2000.

[19] Yusuke Miyao, Kenji Sagae, Rune Sætre, Takuya Matsuzaki, and Jun'ichi Tsujii. Evaluating contributions of natural language parsers to protein–protein interaction extraction. *Bioinformatics*, 25(3):394–400, 2009.

[20] Junkyu Lee, Seongsoon Kim, Sunwon Lee, Kyubum Lee, and Jaewoo Kang. On the efficacy of per-relation basis performance evaluation for PPI extraction and a high-precision rule-based approach. In *BMC medical informatics and decision making*, volume 13, pages 1–12. Springer, 2013.

[21] Kalpana Raja, Suresh Subramani, and Jeyakumar Natarajan. PPInterFinder—a mining tool for extracting causal relations on human proteins from literature. *Database*, 2013, 2013.

[22] Jae-Ho Kim, In-Ho Kang, and Key-Sun Choi. Unsupervised named entity classification models and their ensembles. In *COLING 2002: The 19th International Conference on Computational Linguistics*, 2002.

[23] Payal Chandak, Kexin Huang, and Marinka Zitnik. Building a knowledge graph to enable precision medicine. *Scientific Data*, 10(1):67, 2023.

[24] Lishuang Li, Rongpeng Zhou, and Degen Huang. Two-phase biomedical named entity recognition using CRFs. *Computational biology and chemistry*, 33(4):334–338, 2009.

[25] Rakesh Patra and Sujan Kumar Saha. A Kernel-Based Approach for Biomedical Named Entity Recognition. *The Scientific World Journal*, 2013(1):950796, 2013.

[26] Lixiang Hong, Jinjian Lin, Shuya Li, Fangping Wan, Hui Yang, Tao Jiang, Dan Zhao, and Jianyang Zeng. A novel machine learning framework for automated biomedical relation extraction from large-scale literature repositories. *Nature Machine Intelligence*, 2(6):347–355, 2020.

[27] Hong-Tao Zhang, Min-Lie Huang, and Xiao-Yan Zhu. A unified active learning framework for biomedical relation extraction. *Journal of Computer Science and Technology*, 27(6):1302–1313, 2012.

[28] Peter Corbett and Ann Copestake. Cascaded classifiers for confidence-based chemical named entity recognition. *BMC bioinformatics*, 9:1–10, 2008.

[29] Lindsey Bell, Rajesh Chowdhary, Jun S Liu, Xufeng Niu, and Jinfeng Zhang. Integrated bio-entity network: a system for biological knowledge discovery. *PloS one*, 6(6):e21474, 2011.

[30] Radu Florian, Abe Ittycheriah, Hongyan Jing, and Tong Zhang. Named entity recognition through classifier combination. In *Proceedings of the seventh conference on Natural language learning at HLT-NAACL 2003*, pages 168–171, 2003.

[31] Robert Leaman, Chih-Hsuan Wei, and Zhiyong Lu. tmChem: a high performance approach for chemical named entity recognition and normalization. *Journal of cheminformatics*, 7:1–10, 2015.

[32] Fei Li, Meishan Zhang, Guohong Fu, and Donghong Ji. A neural joint model for entity and relation extraction from biomedical text. *BMC bioinformatics*, 18:1–11, 2017.

[33] Suncong Zheng, Feng Wang, Hongyun Bao, Yuexing Hao, Peng Zhou, and Bo Xu. Joint Extraction of Entities and Relations Based on a Novel Tagging Scheme. In *Proceedings of the 55th Annual Meeting of the Association for Computational Linguistics (Volume 1: Long Papers)*, pages 1227–1236, 2017.

[34] Gamal Crichton, Sampo Pyysalo, Billy Chiu, and Anna Korhonen. A neural network multi-task learning approach to biomedical named entity recognition. *BMC bioinformatics*, 18:1–14, 2017.

[35] Maryam Habibi, Leon Weber, Mariana Neves, David Luis Wiegandt, and Ulf Leser. Deep learning with word embeddings improves biomedical named entity recognition. *Bioinformatics*, 33(14):i37–i48, 2017.

[36] Jinghang Gu, Fuqing Sun, Longhua Qian, and Guodong Zhou. Chemical-induced disease relation extraction via convolutional neural network. *Database*, 2017:bax024, 2017.

[37] Jacob Devlin, Ming-Wei Chang, Kenton Lee, and Kristina Toutanova. Bert: Pre-training of deep bidirectional transformers for language understanding. In *Proceedings of the 2019 conference of the North American chapter of the association for computational linguistics: human language technologies, volume 1 (long and short papers)*, pages 4171–4186, 2019.

[38] Jinhyuk Lee, Wonjin Yoon, Sungdong Kim, Donghyeon Kim, Sunkyu Kim, Chan Ho So, and Jaewoo Kang. BioBERT: a pre-trained biomedical language representation model for biomedical text mining. *Bioinformatics*, 36(4):1234–1240, 2020.

[39] Iz Beltagy, Kyle Lo, and Arman Cohan. SciBERT: A Pretrained Language Model for Scientific Text. In *Proceedings of the 2019 Conference on Empirical Methods in Natural Language Processing and the 9th International Joint Conference on Natural Language Processing (EMNLP-IJCNLP)*, pages 3615–3620, 2019.

[40] Yuan Zhang, Feng Pan, Xin Sui, Donghu Sun, Menghan Chung, and Jinfeng Zhang. Constructing the largest-scale biomedical knowledge graph using all PubMed articles and its application in automated knowledge discovery. *Cancer Research*, 83(7_Supplement):5366–5366, 2023.

[41] Yuan Zhang, Xin Sui, Feng Pan, Kaixian Yu, Keqiao Li, Shubo Tian, Arslan Erdengasileng, Qing Han, Wanjing Wang, Jianan Wang, et al. A comprehensive large-scale biomedical knowledge graph for AI-powered data-driven biomedical research. *Nature Machine Intelligence*, pages 1–13, 2025.

[42] OpenAI. GPT-4 Technical Report, 2023.

[43] OpenAI. Hello GPT-4o, May 2024.

[44] Yanpeng Ye, Jie Ren, Shaozhou Wang, Yuwei Wan, Imran Razzak, Bram Hoex, Haofen Wang, Tong Xie, and Wenjie Zhang. Construction and Application of Materials Knowledge Graph in Multidisciplinary Materials Science via Large Language Model. *Advances in Neural Information Processing Systems*, 37:56878–56897, 2024.

[45] Xuefeng Bai, Song He, Yi Li, Yabo Xie, Xin Zhang, Wenli Du, and Jian-Rong Li. Construction of a knowledge graph for framework material enabled by large language models and its application. *npj Computational Materials*, 11(1):51, 2025.

[46] Rui Yang, Boming Yang, Xinjie Zhao, Fan Gao, Aosong Feng, Sixun Ouyang, Moritz Blum, Tianwei She, Yuang Jiang, Freddy Lecue, et al. Graphusion: A RAG Framework for Scientific Knowledge Graph Construction with a Global Perspective. In *Companion Proceedings of the ACM on Web Conference 2025*, pages 2579–2588, 2025.

[47] Stephen Gilbert, Jakob Nikolas Kather, and Aidan Hogan. Augmented non-hallucinating large language models as medical information curators. *NPJ digital medicine*, 7(1):100, 2024.

[48] Yuqi Zhu, Xiaohan Wang, Jing Chen, Shuofei Qiao, Yixin Ou, Yunzhi Yao, Shumin Deng, Huajun Chen, and Ningyu Zhang. Llms for knowledge graph construction and reasoning: Recent capabilities and future opportunities. *World Wide Web*, 27(5):58, 2024.

[49] Frank Wawrzik, Matthias Plaue, Savan Vekariya, and Christoph Grimm. Customized Information and Domain-centric Knowledge Graph Construction with Large Language Models. *arXiv preprint arXiv:2409.20010*, 2024.

[50] Rui Yang, Boming Yang, Sixun Ouyang, Tianwei She, Aosong Feng, Yuang Jiang, Freddy Lecue, Jinghui Lu, and Irene Li. Graphusion: Leveraging large language models for scientific knowledge graph fusion and construction in nlp education. *arXiv preprint arXiv:2407.10794*, 2024.

[51] Yassir Lairgi, Ludovic Moncla, Rémy Cazabet, Khalid Benabdeslem, and Pierre Cléau. itext2kg: Incremental knowledge graphs construction using large language models. In *International Conference on Web Information Systems Engineering*, pages 214–229. Springer, 2024.

[52] Zirui Guo, Lianghao Xia, Yanhua Yu, Tu Ao, and Chao Huang. Lightrag: Simple and fast retrieval-augmented generation.

[53] Qiang Sun, Yuanyi Luo, and Wenxiao Zhang. Docs2KG: Unified Knowledge Graph Construction from Heterogeneous Documents Assisted by Large Language Models.

[54] Haoyu Huang, Chong Chen, Conghui He, Yang Li, Jiawei Jiang, and Wentao Zhang. Can LLMs be Good Graph Judger for Knowledge Graph Construction? *arXiv preprint arXiv:2411.17388*, 2024.

[55] Stefan Langer, Fabian Neuhaus, and Andreas Nürnberger. CEAR: Automatic construction of a knowledge graph of chemical entities and roles from scientific literature. *arXiv preprint arXiv:2407.21708*, 2024.

[56] Bowen Zhang and Harold Soh. Extract, Define, Canonicalize: An LLM-based Framework for Knowledge Graph Construction. In *Proceedings of the 2024 Conference on Empirical Methods in Natural Language Processing*, pages 9820–9836, 2024.

[57] Yansong Ning and Hao Liu. UrbanKGent: A Unified Large Language Model Agent Framework for Urban Knowledge Graph Construction. In *The Thirty-eighth Annual Conference on Neural Information Processing Systems*.

[58] Jiuzhou Han, Nigel Collier, Wray Buntine, and Ehsan Shareghi. PiVe: Prompting with Iterative Verification Improving Graph-based Generative Capability of LLMs. In *Findings of the Association for Computational Linguistics ACL 2024*, pages 6702–6718, 2024.

[59] Hanzhu Chen, Xu Shen, Qitan Lv, Jie Wang, Xiaoqi Ni, and Jieping Ye. SAC-KG: Exploiting Large Language Models as Skilled Automatic Constructors for Domain Knowledge Graph. In *Proceedings of the 62nd Annual Meeting of the Association for Computational Linguistics (Volume 1: Long Papers)*, pages 4345–4360, 2024.

[60] Vamsi Krishna Kommineni, Birgitta König-Ries, and Sheeba Samuel. From human experts to machines: An LLM supported approach to ontology and knowledge graph construction. *arXiv preprint arXiv:2403.08345*, 2024.

[61] Jiaqi Wang, Yuying Chang, Zhong Li, Ning An, Qi Ma, Lei Hei, Haibo Luo, Yifei Lu, and Feiliang Ren. TechGPT-2.0: A large language model project to solve the task of knowledge graph construction. *arXiv preprint arXiv:2401.04507*, 2024.

[62] Jack Boylan, Shashank Mangla, Dominic Thorn, Demian Gholipour Ghalandari, Parsa Ghaffari, and Chris Hokamp. KGValidator: A Framework for Automatic Validation of Knowledge Graph Construction. *arXiv preprint arXiv:2404.15923*, 2024.

[63] Dawei Li, Shu Yang, Zhen Tan, Jae Baik, Sukwon Yun, Joseph Lee, Aaron Chacko, Bojian Hou, Duy Duong-Tran, Ying Ding, et al. DALK: Dynamic Co-Augmentation of LLMs and KG to answer Alzheimer's Disease Questions with Scientific Literature. In *Findings of the Association for Computational Linguistics: EMNLP 2024*, pages 2187–2205, 2024.

[64] Huaiyuan Ying, Zhengyun Zhao, Yang Zhao, Sihang Zeng, and Sheng Yu. CoRTEx: contrastive learning for representing terms via explanations with applications on constructing biomedical knowledge graphs. *Journal of the American Medical Informatics Association*, 31(9):1912–1920, 2024.

[65] Lang Cao, Jimeng Sun, Adam Cross, et al. An Automatic and End-to-End System for Rare Disease Knowledge Graph Construction Based on Ontology-Enhanced Large Language Models: Development Study. *JMIR Medical Informatics*, 12(1):e60665, 2024.

[66] Hakan T Otal, Stephen V Faraone, and M Abdullah Canbaz. A New Perspective on ADHD Research: Knowledge Graph Construction with LLMs and Network Based Insights. In *International Conference on Complex Networks and Their Applications*, pages 337–349. Springer, 2024.

[67] Linyi Ding, Sizhe Zhou, Jinfeng Xiao, and Jiawei Han. Automated construction of theme-specific knowledge graphs. *arXiv preprint arXiv:2404.19146*, 2024.

[68] Qingxiu Dong, Lei Li, Damai Dai, Ce Zheng, Jingyuan Ma, Rui Li, Heming Xia, Jingjing Xu, Zhiyong Wu, Baobao Chang, et al. A Survey on In-context Learning. In *Proceedings of the 2024 Conference on Empirical Methods in Natural Language Processing*, pages 1107–1128, 2024.

[69] Bowen Gu, Rishi J Desai, Kueiyu Joshua Lin, and Jie Yang. Probabilistic medical predictions of large language models. *npj Digital Medicine*, 7(1):367, 2024.

[70] Qwen Team. Qwen2.5: A Party of Foundation Models, September 2024.

[71] Xuezhi Wang, Jason Wei, Dale Schuurmans, Quoc V Le, Ed H Chi, Sharan Narang, Aakanksha Chowdhery, and Denny Zhou. Self-Consistency Improves Chain of Thought Reasoning in Language Models. In *The Eleventh International Conference on Learning Representations*.

[72] Amir Taubenfeld, Tom Sheffer, Eran Ofek, Amir Feder, Ariel Goldstein, Zorik Gekhman, and Gal Yona. Confidence improves self-consistency in llms. *arXiv preprint arXiv:2502.06233*, 2025.

[73] Xinyun Chen, Renat Aksitov, Uri Alon, Jie Ren, Kefan Xiao, Pengcheng Yin, Sushant Prakash, Charles Sutton, Xuezhi Wang, and Denny Zhou. Universal Self-Consistency for Large Language Models. In *ICML 2024 Workshop on In-Context Learning*.

[74] OpenAI. Introducing GPT-4.1 in the API, April 2025.

[75] Aixin Liu, Bei Feng, Bing Xue, Bingxuan Wang, Bochao Wu, Chengda Lu, Chenggang Zhao, Chengqi Deng, Chenyu Zhang, Chong Ruan, et al. Deepseek-v3 technical report. *arXiv preprint arXiv:2412.19437*, 2024.

[76] Guangzhi Xiong, Qiao Jin, Zhiyong Lu, and Aidong Zhang. Benchmarking retrieval-augmented generation for medicine. In *Findings of the Association for Computational Linguistics ACL 2024*, pages 6233–6251, 2024.

[77] Xiaorui Su, Yibo Wang, Shanghua Gao, Xiaolong Liu, Valentina Giunchiglia, Djork-Arné Clevert, and Marinka Zitnik. KGARevion: an AI agent for knowledge-intensive biomedical QA. In *ICLR*, 2025.

[78] OpenAI. New embedding models and API updates, January 2024.

[79] An Yang, Anfeng Li, Baosong Yang, Beichen Zhang, Binyuan Hui, Bo Zheng, Bowen Yu, Chang Gao, Chengen Huang, Chenxu Lv, et al. Qwen3 technical report. *arXiv preprint arXiv:2505.09388*, 2025.

[80] Chih-Hsuan Wei, Alexis Allot, Po-Ting Lai, Robert Leaman, Shubo Tian, Ling Luo, Qiao Jin, Zhizheng Wang, Qingyu Chen, and Zhiyong Lu. PubTator 3.0: an AI-powered literature resource for unlocking biomedical knowledge. *Nucleic Acids Research*, 52(W1):W540–W546, 2024.

[81] Yu Gu, Robert Tinn, Hao Cheng, Michael Lucas, Naoto Usuyama, Xiaodong Liu, Tristan Naumann, Jianfeng Gao, and Hoifung Poon. Domain-Specific Language Model Pretraining for Biomedical Natural Language Processing, 2020.

[82] Mary L McHugh. Interrater reliability: the kappa statistic. *Biochemia medica*, 22(3):276–282, 2012.

[83] J. Richard Landis and Gary G Koch. The measurement of observer agreement for categorical data. *Biometrics*, 33(1):159–174, 1977.

[84] Jiageng Wu, Bowen Gu, Ren Zhou, Kevin Xie, Doug Snyder, Yixing Jiang, Valentina Carducci, Richard Wyss, Rishi J Desai, Emily Alsentzer, et al. BRIDGE: Benchmarking Large Language Models for Understanding Real-world Clinical Practice Text. *arXiv preprint arXiv:2504.19467*, 2025.

[85] Zhong-Zhi Li, Duzhen Zhang, Ming-Liang Zhang, Jiaxin Zhang, Zengyan Liu, Yuxuan Yao, Haotian Xu, Junhao Zheng, Pei-Jie Wang, Xiuyi Chen, et al. From system 1 to system 2: A survey of reasoning large language models. *arXiv preprint arXiv:2502.17419*, 2025.

[86] Yilin Wen, Zifeng Wang, and Jimeng Sun. MindMap: Knowledge Graph Prompting Sparks Graph of Thoughts in Large Language Models. In *Proceedings of the 62nd Annual Meeting of the Association for Computational Linguistics (Volume 1: Long Papers)*, pages 10370–10388, 2024.

[87] Siye Wu, Jian Xie, Jiangjie Chen, Tinghui Zhu, Kai Zhang, and Yanghua Xiao. How Easily do Irrelevant Inputs Skew the Responses of Large Language Models? In *First Conference on Language Modeling*.

[88] Weiwei Sun, Lingyong Yan, Xinyu Ma, Shuaiqiang Wang, Pengjie Ren, Zhumin Chen, Dawei Yin, and Zhaochun Ren. Is ChatGPT Good at Search? Investigating Large Language Models as Re-Ranking Agents. In *Proceedings of the 2023 Conference on Empirical Methods in Natural Language Processing*, pages 14918–14937, 2023.

7 Author contributions

D.Z. conceived the method, collected and pre-processed the data, implemented the core MedKGent framework, constructed the KG, and wrote the manuscript. Z.W. performed automatic quality assessment of the extracted relational triples, evaluated downstream utility in medical QA, and conducted qualitative analysis on literature-based drug repurposing cases. Z.L. was responsible for deploying the LLM API and optimizing the efficiency of relational triple extraction. Y.Y. and S.J. contributed to the preparation of figures and data visualization. H.X. and X.W. provided the GPU resources for API deployment and offered guidance on optimization and acceleration. J.D., Y.Z., T.Z. and J.Y. served as intermittent advisors, offering suggestions on experimental design and manuscript writing. X.C. and L.S. designed the overall study, served as corresponding authors, and played a key role in coordinating and integrating all resources. All the authors read and approved the manuscript.

8 Competing interests

The authors declare no competing interests.